



A Review of FE-FFT-Based Two-Scale Methods for Computational Modeling of Microstructure Evolution and Macroscopic Material Behavior

Christian Gierden¹ · Julian Kochmann² · Johanna Waimann¹ · Bob Svendsen^{3,4} · Stefanie Reese¹

Received: 25 May 2021 / Accepted: 28 February 2022
© The Author(s) 2022

Abstract

The overall, macroscopic constitutive behavior of most materials of technological importance such as fiber-reinforced composites or polycrystals is very much influenced by the underlying microstructure. The latter is usually complex and heterogeneous in nature, where each phase constituent is governed by non-linear constitutive relations. In order to capture such micro-structural characteristics, numerical two-scale methods are often used. The purpose of the current work is to provide an overview of state-of-the-art finite element (FE) and FFT-based two-scale computational modeling of microstructure evolution and macroscopic material behavior. Spahn et al. (Comput Methods Appl Mech Eng 268:871–883, 2014) were the first to introduce this kind of FE-FFT-based methodology, which has emerged as an efficient and accurate tool to model complex materials across the scales in the recent years.

1 Introduction

At small length scales, most materials are heterogeneous, such as composites, porous media, or polycrystalline aggregates. Accordingly, e.g. polycrystals are composed of several grains which might vary in spatial distribution, size, morphology and crystallographic orientation. In addition, one grain could also consist of a phase mixture. The related heterogeneous structure has a great impact on the microstructural effects and thus results in more complex non-linear constitutive relations. Examples are grain-wise elasto-viscoplastic material behavior or ductile damage behavior related to the grain boundaries. The material behavior's complexity is increased by microstructural changes which influence the grain's structure, such as martensitic phase transformations

and dynamic recrystallization; see Fig. 1. These effects make it even more difficult to establish appropriate overall constitutive relations to describe the material behavior. Instead of finding such a phenomenological expression, a multiscale approach enables to separately examine the different scales. Within a two-scale simulation approach, the macroscale is used to capture the overall boundary value problem including the external boundary conditions. Meanwhile, the material behavior at the macroscale is determined by the mean response of the smaller scale (microscale). Various methods have been developed to capture the structure, properties and physical behavior of the microstructure and its overall constitutive response. These so-called multiscale schemes may be classified in three major groups: (semi-)analytical methods [169, 214], computational methods [194, 196] and hybrid methods [45, 130].

The focus of the present paper is on one particular computational two-scale technique, namely the FE-FFT-based method. This methodology was first proposed by Spahn et al. [196] and serves as an efficient and powerful alternative compared to the classical computational homogenization method, the FE² method [129, 144, 167]. The FE-FFT-based method includes a finite element (FE) approach for the macroscale simulation and an evaluation of the behavior at the microscale based on fast Fourier transforms (FFT). The macroscopic material behavior is then defined as volume average of its microscopic counterpart. While the FE approach is

✉ Christian Gierden
christian.gierden@rwth-aachen.de

¹ Institute of Applied Mechanics, RWTH Aachen University, 52074 Aachen, Germany

² MTU Aero Engines AG, 80995 Munich, Germany

³ Material Mechanics, RWTH Aachen University, 52062 Aachen, Germany

⁴ Microstructure Physics and Alloy Design, Max-Planck-Institut für Eisenforschung GmbH, 40237 Düsseldorf, Germany

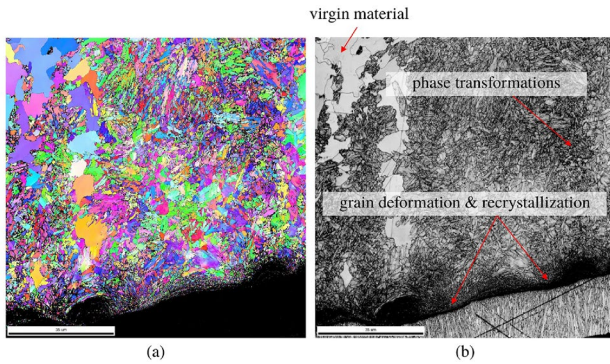


Fig. 1 Ferrite/pearlite-annealed 42CrMo4 steel microstructure: **a** inverse pole figure illustrating the grain orientations and **b** image quality map obtained from EBSD measurements illustrating microstructural grain changes, such as phase transformations and recrystallization [99]

widely used in terms of computational mechanics, the FFT-based method is rather new and was introduced by Moulinec and Suquet [155, 156]. It serves as alternative to the classical FE-based simulation of periodic microstructures and is based on solving a global integral equation known as the Lippmann–Schwinger equation [107, 228], which is defined by Green’s function and a polarization stress.

The review paper is structured as follows: after a brief review of the three groups of multiscale techniques (Sect. 2), a review of the FFT-based microstructure simulation is given in Sect. 3. This includes a brief summary of FFT-based algorithms (Sects. 3.2 and 3.3), FFT-based model-order reduction techniques (Sect. 3.4), as well as the applications of the FFT-based simulation (Sect. 3.5). In addition a brief comparison of the FFT-based method to the FE-based method is given in Sect. 3.6. Finally, in Sect. 4, the FE-FFT-based two-scale method is discussed for different applications. The paper ends with a conclusion in Sect. 5.

2 Overview of Multiscale Methods

Figure 2 presents the key idea of a multiscale approach in terms of a mechanical boundary value problem considering small strain kinematics. On the macroscale the macroscopic strain $\bar{\varepsilon}(\bar{x})$ at the macroscopic position \bar{x} is computed. This macroscopic strain is used on the microscale to compute the overall strain $\varepsilon(\bar{x}, \mathbf{x})$ and stress $\sigma(\bar{x}, \mathbf{x})$ response. In terms of a spatially resolved microstructure simulation, \mathbf{x} represents the microscopic position. Vice versa, the resulting macroscopic stress $\bar{\sigma}(\bar{x})$ and macroscopic tangent operator $\bar{\mathbb{C}}(\bar{x})$ are defined as volume averages of their overall counterparts.

Besides this two-scale method, also multiscale methods incorporating more than two scales (for example all the way down to the atomistic level, [170]) exist. Nevertheless we

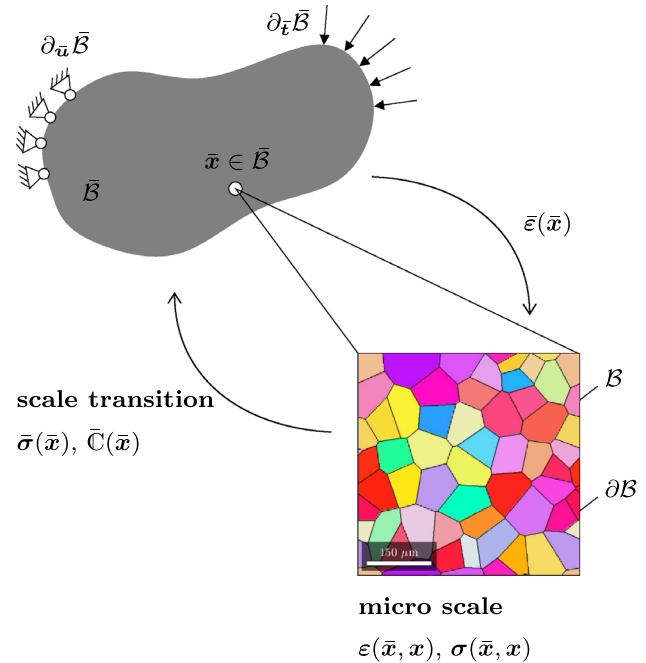


Fig. 2 Schematic of the two-scale simulation approach incorporating a polycrystalline microstructure

restrict ourselves exclusively to the two-scale method. Doing that, Table 1 and the following three subsections briefly summarize the three different classifications of two-scale methods, the (semi-)analytical, the computational and the hybrid method.

2.1 (Semi-)Analytical Methods

In analytical methods, a deterministic or statistical representation of the microstructure is used. Often, closed form solutions of reference problems serve to compute the overall response of microscopic heterogeneous materials. If an explicit solution for the material behavior is not available but approximated by implicit equations, the method is called a semi-analytical method. In both cases, a spatially resolved visualization of the results on the microscale is not possible.

First attempts to compute the overall macroscopic material behavior of microscopic heterogeneous materials in terms of an analytical homogenization were established by Voigt [214] and Reuss [169]. Whereby Voigt assumes that the strain is constant within the microstructure, resulting in an overall stiffness tensor computed by using the arithmetic mean of the phase-wise stiffness tensor weighted by the corresponding volume fraction, Reuss considers a constant stress in the individual phases. This ansatz results in the computation of the arithmetic mean of the phase-wise compliance tensors again weighted by the corresponding volume fractions. These basic analytical homogenization methods

Table 1 Classification of the three major different two-scale methods

(Semi-)analytical methods	Hybrid methods	Computational methods
Arithmetic and harmonic mean [169, 214]	TFA/NTFA [45, 60, 141]	FE ² method [58, 63, 194]
Eshelby solution [54, 84, 153]	Clustering analysis [130, 231]	FE-FFT method [100, 196, 206]
Variational approach [81–83]		

are called “mean field methods”. In the context of statistical methods, the volume fractions of the different phases can be interpreted as first order correlation functions. Since these basic approximations are only related to the volume fractions of certain phases, they are not very accurate in general, but still serve as upper and lower bounds of the averaged material response in terms of homogenization methods. Regarding polycrystalline materials, these bounds are often referred to as the Taylor [203] and Sachs [177] bounds. To generate more accurate homogenized results, the use of a two-point or higher-order correlation function enables the consideration of additional microstructural details [55, 205].

The work of Eshelby [54] deals with an ellipsoidal elastic inclusion embedded in a homogeneous infinite matrix. The present analytic solution for the so-called Eshelby’s inclusion serves as the basis for different more precise mean field approaches [159], such as the Mori-Tanaka model [153] or the double inclusion method introduced in [127]. Furthermore, a self-consistent approximation was introduced in [21, 84, 86, 106] for the simulation of elastic composites and polycrystals. Within this self-consistent approach it is assumed that the material properties of the homogeneous infinite matrix coincide with the overall properties of the composite. An extension of this approach to the computation of the overall properties of non-linear composites is given in [27, 200] and of non-linear polycrystals in [87, 96, 97, 116, 151, 187].

A variational approach for the estimation of the behavior of linear composites with an isotropic microstructure was introduced by Hashin and Shtrikman [81–83, 91]. This approach is still based on the assumption of phase-wise constant fields, but in addition the stress state consists of two parts. One part is related to a homogenous reference material and the other part is related to a polarization stress which characterizes the fluctuation within the microstructure. The resulting inhomogeneous partial differential equation is solved by use of Green’s function [158, 197] and hence, yields an integral formulation known as Lippmann–Schwinger equation [107, 228]. For homogeneous and isotropic reference materials which behave elastically, closed-form solutions for the Lippmann–Schwinger equation are available. Compared to the Voigt and Reuss bounds, which do not consider the fluctuation of the stress on the microscale, this variational approach leads to stricter bounds

in terms of the overall response of the microstructural material behavior. An extension of the ansatz to anisotropic composites is given in [227] and to non-linear composites in [30, 80, 199, 228]. To further improve the accuracy of the application of the analytical homogenization on microstructures with large variations in their local properties, also second-order homogenization techniques based on incorporating field fluctuations have been proposed in [28, 29, 37, 195].

2.2 Computational Methods

In contrast to (semi-)analytical methods, a computational multiscale method deals with a spatially resolved representation of the microstructure. In this context, the microstructure might be seen as a representative volume element (RVE) and/or unit cell, [44, 80, 85, 161], or a statistically similar RVE, [5, 185]. The macroscopic kinematics serve as an input for the RVE and thus influence the deformation of the microstructure. The macroscopic influence can be prescribed by different possible boundary conditions, such as linear displacements, constant tractions, or combined periodic displacements and anti periodic tractions, [105, 204, 210].

The most common method to solve the related microscopic boundary value problem (BVP) is the finite element method [8, 237]. The performed computational simulation leads to spatially resolved representations of the microstructural fields, like the stress and the strain fields. Accordingly, the volume average of the local microscopic fields determines the required overall macroscopic response, see [85, 137]. Two-scale approaches which use the finite element method to calculate the BVPs on the micro-level as well as on the macro-level are called FE² methods [58, 194]. To calculate the required overall algorithmic tangent operator closed form expressions were derived in [148, 149]. An overview of recent developments, applications and challenges concerning the FE² method can be found in [63, 186].

Other microstructural methods in terms of a two-scale full field simulation are for example finite differences (FD)-based [1], Voronoi FE-based [65], virtual element-based [4, 139] and FFT-based solvers [196]. Among these methods, the FFT-based method has proven to be a fast and accurate tool in terms of a computational simulation of periodic microstructures in the recent years. An overview of recent

developments, applications and challenges concerning the FFT-based microstructure simulation [155, 156] and the related FE-FFT-based two-scale method [100, 196] is given in Sects. 3 and 4, respectively.

A comparison of the aforementioned analytical and numerical methods is presented in [88, 120]. Concerning the computational methods, Sect. 3.6 gives a brief comparison of the FE- and FFT-based microstructure simulation.

2.3 Hybrid Methods

Hybrid multiscale methods finally combine both, computationally efficient numerical methodologies and theoretical knowledge. In particular, numerical experiments, such as deforming a highly resolved microstructure incorporating different loading conditions, are performed in a pre-processing step to generate microstructural data, such as the point-wise material behavior related to the external loading. Then, the obtained information about the microstructural material behavior is used for the actual micro-mechanical modeling.

In this context, one methodology is the uniform transformation field analysis (TFA) [45, 59]. It is based on the assumption of piece-wise uniform plastic strain fields to reduce the degrees of freedom during the simulation. Therefore a significant reduction of computational time is gained. A generalization of this method in terms of the non-uniform TFA (NTFA) is given in [60, 61, 141–143]. Instead of considering uniform plastic strain fields, the latter quantities are decomposed into a set of plastic modes, which leads to nonuniform plastic strain fields. These modes have to be computed within a pre-processing step. Nevertheless, also the NTFA leads to a highly reduced set of constitutive equations, which again results in a significant reduction of the computational costs.

Another recently developed hybrid multiscale method is the self-consistent clustering analysis (SCA) [31, 130,

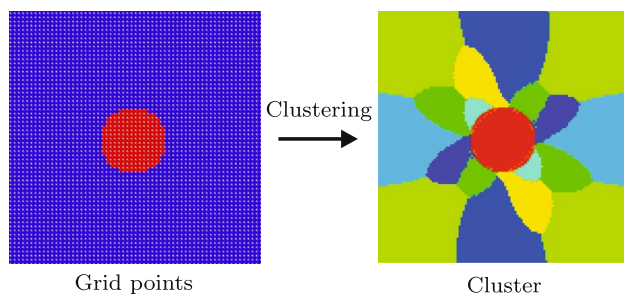


Fig. 3 Highly resolved two-phase microstructure with a point-wise material behavior, while the inclusion is colored red and matrix is colored blue (*left*) and clustered microstructure with a cluster-wise constant material behavior, while each color represents one cluster (*right*) (Colour figure online)

[131, 221, 231]. This method is derived from the Lippmann–Schwinger equation [107, 228] and based on a clustered microstructure with cluster-wise constant micromechanical fields. A pre-processing step is used to group the highly resolved material behavior into these clusters, see Fig. 3. Under the assumption of constant stress and strain fields during the actual simulation, a significant reduction of degrees of freedom and also a significant reduction of computational times compared to a full field computational two-scale simulation is gained. A generalization of the SCA to finite strain kinematics is given in [232].

3 FFT-Based Microstructure Simulation

The FFT-based microstructure simulation is used in terms of a spatially resolved microstructure simulation. Initially, it was introduced by Moulinec and Suquet based on fixed-point iterations [155, 156]. This basic fixed-point scheme is reviewed in Sect. 3.1. It is followed by an overview of several more efficient FFT-based algorithms and solution methods (Sect. 3.2) and Sect. 3.3, discussing problems related to the Gibbs phenomenon. In addition, recently introduced model order reduction techniques for the FFT-based method are reviewed in Sect. 3.4. Subsequently, Sect. 3.5 provides an overview of different applications of the FFT-based method for the simulation of composite (Sect. 3.5.1) and polycrystalline (Sect. 3.5.2) microstructures, respectively. Finally, a brief comparison to the FE-based microstructure simulation is given in Sect. 3.6. A recapitulation of the FFT-based algorithms, solvers and their applications is also given in Table 2.

3.1 Basic Fixed-Point Scheme

In terms of a spatially resolved microstructure simulation of a mechanical boundary value problem considering small strain kinematics, the overall strain $\epsilon(\bar{\mathbf{x}}, \mathbf{x})$ is additively split into the macroscopic part $\bar{\epsilon}(\bar{\mathbf{x}})$ (see Fig. 2) and a microscopic fluctuating part $\tilde{\epsilon}(\mathbf{x})$, see Fig. 4. Since the balance of linear momentum holds for the macroscopic as well as for the microscopic scale, the microstructural mechanical boundary value problem is captured by

$$\begin{aligned} \operatorname{div} \boldsymbol{\sigma}(\bar{\mathbf{x}}, \mathbf{x}) &= \mathbf{0} \\ \boldsymbol{\sigma}(\bar{\mathbf{x}}, \mathbf{x}) &= \boldsymbol{\sigma}(\bar{\mathbf{x}}, \mathbf{x}, \epsilon(\bar{\mathbf{x}}, \mathbf{x}), \boldsymbol{\alpha}(\bar{\mathbf{x}}, \mathbf{x})) \\ \epsilon(\bar{\mathbf{x}}, \mathbf{x}) &= \bar{\epsilon}(\bar{\mathbf{x}}) + \tilde{\epsilon}(\mathbf{x}). \end{aligned} \quad (1)$$

Thereby, $\operatorname{div}(\cdot)$ represents the divergence operator and the total stress field $\boldsymbol{\sigma}(\bar{\mathbf{x}}, \mathbf{x})$ depends on the macroscopic position $\bar{\mathbf{x}}$, the microscopic position \mathbf{x} , the related total strain field $\epsilon(\bar{\mathbf{x}}, \mathbf{x})$ as well as—related to the observed problem—on some internal variables $\boldsymbol{\alpha}(\bar{\mathbf{x}}, \mathbf{x})$, e.g. the plastic strain and/

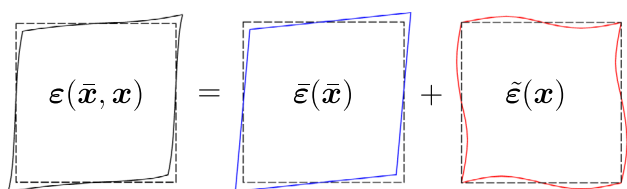


Fig. 4 Additive split of the total strain into the constant macroscopic part and the fluctuating microscopic part

or a grain orientation. Body forces are neglected within the microscopic BVP since they are already considered within the macroscopic BVP.

Considering periodic fields and boundary conditions, the microscopic boundary value problem may be solved using spectral methods [125, 158, 159]. Therefore, the inhomogeneous BVP with varying material properties, see Fig. 5 (left), is reformulated as equivalent homogeneous BVP by introducing a microstructure with a homogeneous reference material behavior C^0 , see Fig. 5 (right). Doing this, the equivalent homogeneous BVP reads

$$\begin{aligned} \text{div}[C^0 : \epsilon(\bar{x}, \mathbf{x})] &= -\text{div}[\boldsymbol{\tau}(\bar{x}, \mathbf{x})] \\ \boldsymbol{\tau}(\bar{x}, \mathbf{x}) &:= \boldsymbol{\sigma}(\bar{x}, \mathbf{x}) - C^0 : \epsilon(\bar{x}, \mathbf{x}) \\ \epsilon(\bar{x}, \mathbf{x}) &= \bar{\epsilon}(\bar{x}) + \tilde{\epsilon}(\mathbf{x}), \end{aligned} \tag{2}$$

where $\boldsymbol{\tau}(\bar{x}, \mathbf{x})$ is the so-called polarization stress, which represents the material inhomogeneities within the homogeneous reference material behavior.

Equation (2) may be solved by using Green’s function $G^0(\mathbf{x} - \mathbf{x}')$ or the Lippmann–Schwinger operator $\Gamma^0(\mathbf{x} - \mathbf{x}')$ [158, 197], respectively, which yields to an integral form known as the Lippmann–Schwinger equation [107, 228]:

$$\epsilon(\bar{x}, \mathbf{x}) = \bar{\epsilon}(\bar{x}) - \int_{\Omega} \Gamma^0(\mathbf{x} - \mathbf{x}') : \boldsymbol{\tau}(\mathbf{x}') \, d\mathbf{x}' \tag{3}$$

or in a compact notation:

$$\epsilon = \bar{\epsilon} - \Gamma^0 * \boldsymbol{\tau}. \tag{4}$$

Within Eq. (3) \mathbf{x} and \mathbf{x}' represent different positions within the microstructural domain Ω with the side length L , while $*$ represents the convolution integral in Eq. (4).

The Lippmann–Schwinger equation is solved by transferring it into Fourier space yielding:

$$\hat{\epsilon}(\boldsymbol{\xi}) = \begin{cases} -\hat{\Gamma}^0(\boldsymbol{\xi}) \hat{\boldsymbol{\tau}}(\boldsymbol{\xi}) & \forall \boldsymbol{\xi} \neq \mathbf{0} \\ \bar{\epsilon}(\bar{x}) & \forall \boldsymbol{\xi} = \mathbf{0} \end{cases}, \tag{5}$$

while (\cdot) refers to the Fourier representation of the corresponding field depending on the wave vector $\boldsymbol{\xi}$, which

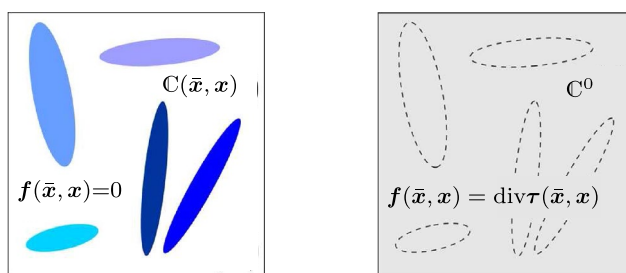


Fig. 5 Left Inhomogeneous microstructure with spatially varying material properties, such as a spatially depending stiffness tensor $C(\bar{x}, \mathbf{x})$, while body forces are neglected. Right Homogeneous reference microstructure with a constant reference material behavior C^0 , while the inhomogeneities are described in terms of the body force $f(\bar{x}, \mathbf{x}) = \text{div}\boldsymbol{\tau}(\bar{x}, \mathbf{x})$

gathers all the considered Fourier modes. The components $\xi_j (j = 1, 2, 3)$ of this wave vector are defined as

$$\xi_j(i) = \frac{2\pi}{L} i \quad \text{with} \quad i = -\frac{N}{2}, \dots, \frac{N}{2} - 1 \tag{6}$$

for a discretized microstructure with an even number of grid points N and

$$\xi_j(i) = \frac{2\pi}{L} i \quad \text{with} \quad i = -\frac{N-1}{2}, \dots, \frac{N-1}{2} \tag{7}$$

for a discretized microstructure with an odd number of grid points N .

In Fourier space, Green’s function $\hat{G}^0(\boldsymbol{\xi})$ and the Lippmann–Schwinger operator $\hat{\Gamma}^0(\boldsymbol{\xi})$ are explicitly known and just depending on this wave vector and the homogeneous reference material behavior C^0 :

$$\hat{G}_{ki}^0(\boldsymbol{\xi}) = \left(C_{kjil}^0 \xi_l \xi_j \right)^{-1} \tag{8}$$

and

$$\begin{aligned} \hat{\Gamma}_{ijkl}^0(\boldsymbol{\xi}) &= \frac{1}{4} \left(\hat{G}_{jk,li}^0(\boldsymbol{\xi}) + \hat{G}_{ik,lj}^0(\boldsymbol{\xi}) + \hat{G}_{jl,ki}^0(\boldsymbol{\xi}) + \hat{G}_{il,kj}^0(\boldsymbol{\xi}) \right). \end{aligned} \tag{9}$$

The basic fixed-point iteration scheme for the FFT-based microstructure simulation, which makes use of the Fourier representation of the Lippmann–Schwinger equation (5) and the computation of the polarization stress $\boldsymbol{\tau}(\bar{x}, \mathbf{x})$ in real space (Equation (2)) was introduced by Moulinec and Suquet [155, 156].

Table 2 FFT-based numerical solution methods and applications

Algorithms, solvers, and applications	Key references
FFT-based algorithms	
Basic and related schemes	Moulinec and Suquet [155–157], Dreyer and Müller [43], Lebensohn [112], Lahellec et al. [110], Eisenlohr et al. [49], Kabel et al. [92]
Polarization-based scheme	Eyre and Milton [56], Michel et al. [146], Moulinec and Suquet [157], Vinogradov and Milton [213], Monchiet and Bonnet [152], Moulinec and Silva [154], Schneider et al. [184]
Scheme based on augmented Lagrangians	Michel et al. [145, 146], Moulinec and Suquet [157], Lebensohn et al. [122], Moulinec and Silva [154]
Scheme based on discrete Green's operator	Jacques [90], Eloh et al. [51, 52], Berbenni et al. [10], Khorrami et al. [95]
Fourier–Galerkin approach	Bonnet [17], Brisard and Dormieux [19, 20], Vondřejc et al. [218, 219], Vondřejc [216], Zeman et al. [234], Geus et al. [38]
Solution methods	
Fixed-point scheme	Moulinec and Suquet [155, 156], Eisenlohr et al. [49], Eyre and Milton [56], Michel et al. [145, 146], Schneider et al. [184], Lebensohn et al. [122]
Conjugate and fast gradient solver	Zeman et al. [233], Brisard and Dormieux [19, 20], Vondřejc et al. [218], Gélébart and Mondon-Cancel [64], Kabel et al. [92], Schneider [179]
Quasi-Newton method	Shanthraj et al. [189], Schneider [180], Chen et al. [34, 35], Wicht et al. [226]
Using high performance computing	Eghtesad et al. [46], Grimm-Strele and Kabel [76], Eghtesad and Knezevic [48], Eghtesad et al. [47]
Methods to reduce the effect of Gibbs oscillations on convergence behavior	Willot et al. [230], Berbenni et al. [9], Willot [229], Lebensohn and Needleman [113], Schneider et al. [182, 183], Vidyasagar et al. [211, 212], Anglin et al. [3], Kabel et al. [93], Eloh et al. [52], Khorrami et al. [95], Leute et al. [124]
Incorporating MOR techniques	Garcia-Cardona et al. [62], Kochmann et al. [104], Gierden et al. [68, 70, 71], Vondřejc et al. [220]
Simulation of composite microstructures	
Composites with finite phase contrast	Moulinec and Suquet [155, 156], Eyre and Milton [56], Lahellec et al. [110], Vinogradov and Milton [213], Šmilauer and Bažant [193], Zeman et al. [233], Lavergne et al. [111], Ostrowski et al. [162]
Composites with infinite phase contrast	Michel et al. [145], Bilger et al. [14], Bilger et al. [15], Brisard and Dormieux [19], Monchiet and Bonnet [152], Ghosseinr and Lévesque [66], Vondřejc et al. [218], Gélébart and Mondon-Cancel [64], Kabel et al. [92], Schneider [179, 180], Wicht et al. [226], Charière et al. [32], Görthofer et al. [74]
Damage, fracture and fatigue behavior	Spahn et al. [196], Sliseris et al. [192], Boeff et al. [16], Wang et al. [222], Li et al. [126], Chen et al. [34, 35], Ernesti et al. [53], Cao et al. [25], Ma and Sun [135], Magri et al. [136], Köbler [98]
Simulation of polycrystalline microstructures	
Rigid-viscoplastic polycrystals	Lebensohn [112], Lebensohn et al. [118], Rollett et al. [171], Lee et al. [114]
Elasto-viscoplastic polycrystals (EVP)	Lebensohn et al. [122, 123], Eisenlohr et al. [49], Kanjarla et al. [94], Roters et al. [174], Diehl et al. [41], Ozturk and Rollett [163], Cantara et al. [24], Niezgodna et al. [160], Kumar et al. [108, 109], Cunningham et al. [36], Roters et al. [172]
EVP coupled with a phase field model	Chen et al. [33], Zhao et al. [236], Kochmann et al. [100], Roters et al. [172], Ma and Sun [135]
EVP coupled with dislocation dynamics	Berbenni et al. [9, 10], Djaka et al. [42], Bertin et al. [12], Santos et al. [178], Bertin and Capolungo [11]
Damage, fracture and fatigue behavior	Rovinelli et al. [175, 176], Sharma et al. [190, 191], Roters et al. [172], Ma and Sun [135], Lucarini et al. [133], Mareau [138]
Comparison to FE-based simulations	Michel et al. [144], Prakash and Lebensohn [167], Liu et al. [129], El Shawish et al. [50], Vondřejc and Geus [217]

3.2 Overview and Efficiency of FFT-Based Algorithms and Solution Methods

Recently, two review papers on FFT-based algorithms, solution methods and their applications were published by Schneider [181] and Lucarini et al. [134]. Nevertheless, this subsection briefly sums up the most important developments in this context.

The works presented in [43, 112, 155, 156] deal with the FFT-based basic fixed point scheme for small strain kinematics, reviewed in Sect. 3.1. The generalization of this method to finite strain kinematics is presented in [49, 110]. The rate of convergence of the basic fixed point scheme depends on the contrast between the phases, the choice for the homogeneous reference material behavior, and the material behavior itself (linear or non-linear). While different choices for the homogeneous reference material behavior are generally possible, the best convergence behavior for the fixed point scheme is gained by the arithmetic averages of the phase-dependent Lamé coefficients λ^0 and μ^0 [92, 156].

Independent of the choice for the reference material behavior, the convergence for the simulation of materials with high phase contrast is very slow and not even ensured for an infinite phase contrast. Improvements concerning the convergence behavior in this context are achieved by a polarization-based solution scheme [56, 146, 213] and a solution scheme based on augmented Lagrangians [122, 145, 146]. These methods are also called accelerated methods. While the polarization-based scheme relies on a reformulation of the Lippmann–Schwinger equation, the scheme based on augmented Lagrangians yields a reformulation of the microscopic BVP in terms of a minimization problem. A comparison of both methods with each other and to the basic fixed point scheme is given in [157]: For a low phase contrast the CPU time of the basic scheme is the shortest. For higher differences between the constituents, the accelerated schemes, are comparable, while the polarization-based scheme suffers at infinite phase contrast. A generalization of the polarization-based solution scheme for the simulation of composites with infinite phase contrast is given in [152]. A comparison of this general scheme to the initially proposed polarization-based scheme and to the solution scheme based on augmented Lagrangians shows, that the initially proposed polarization-based scheme and the solution scheme based on augmented Lagrangians are particular cases of this general polarization-based scheme [154]. Recently, a review of the polarization based schemes including an extension to the simulation of non-linear material behavior was given in [184].

A further accelerated solution strategy based on a conjugate gradient solver was introduced in [233] with a similar convergence behavior as the previous accelerated methods. This solution strategy is based on a linearized

Lippmann–Schwinger equation (3). Solving the resulting system of linear equations, the gradient decent method may be used. Using conjugate gradients in this context yields an Krylov subspace method, which is an efficient solution strategy of solving the system of linear equations. This first attempt on FFT-based conjugate gradient solvers suffers at infinite phase contrasts but has the advantage that it is independent of the choice for the reference material behavior. Another solution strategy incorporating the conjugate gradient solver [19], is based on a variational framework which minimizes the energy of Hashin and Shtrikman [82]. This solution scheme also leads to convergence in the case of infinite phase contrast and is compared to the basic fixed point scheme in [20]. A further variational framework, based on a Galerkin discretization of the weak form of the microscopic boundary value problem with trigonometric polynomials, is given in [218]. The extension of the conjugate gradient based solver to capture non-linear material behavior is introduced in [64] and to finite strain kinematics in [92]. In addition, the equivalence of the basic fixed point scheme and a gradient descent method is shown in [92].

For complex material behavior, such as plasticity or damage, the conjugacy of the decent directions might get destroyed, so that the conjugate gradient solver will not converge anymore. Due to that, more stable solution strategies based on the non-linear generalized minimal residual method (GMRES) [189] or the fast gradient method of Nesterov [179] were developed. Recently, also a Barzilai–Borwein basic scheme [180] considering the Barzilai–Borwein step size selection technique for the gradient descent and a FFT-based solution scheme based on the heavy-ball method [53] were introduced. Furthermore, a Quasi-Newton method for a tangent-free FFT-based simulation of a complex non-linear material behavior is presented in [226]. Besides the investigations of these algorithms in the primal formulation of the unit cell problem, the effects of these solvers in a dual formulation [13] are investigated in [225].

Supplementary to the focus on computational efficiency, all these current developments also focus on a memory efficient implementation.

In addition, recent developments deal with the parallel implementation of these solvers using Message Passing Interface (MPI) and OpenMP [46, 76], or high-performance computational platforms integrating a graphics processing unit (GPU) [47, 48].

3.3 Methods to Reduce the Effect of Gibbs Oscillations on Convergence Behavior

Concerning the FFT-based simulations, well known numerical artifacts are oscillations around discontinuities, known as the Gibbs phenomenon [67]. Approaches to tackle this problem use for example a modified Lippmann–Schwinger

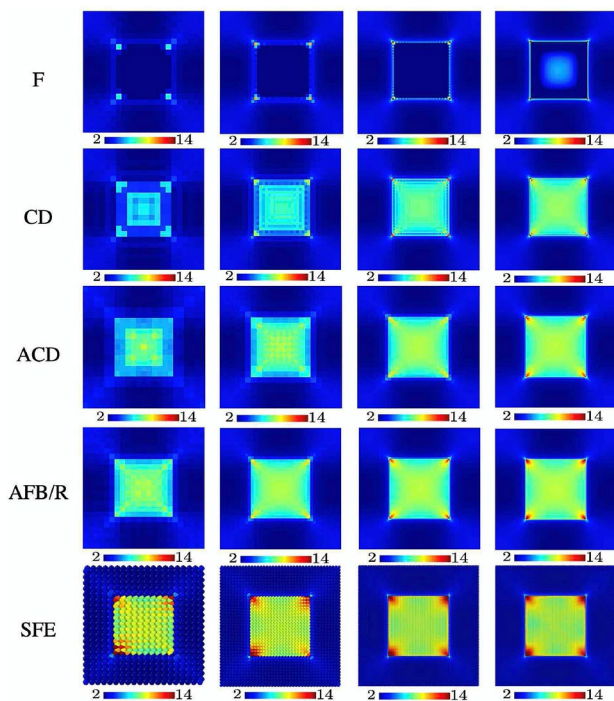


Fig. 6 Results for the isotropic linear elastic 3D shear stress field σ_{12}/μ_M (x_1 horizontal, x_2 vertical, μ_M matrix shear modulus) obtained from different algorithms at a matrix–inclusion interface with discontinuous elastic stiffness phase contrast of 1000 for different spectral algorithms and different 3D numerical resolutions n^3 with $n = 22$ (left), $n = 42$ (middle left), $n = 82$ (middle right), and $n = 162$ (right). Compared here are algorithms employing finite-difference discretization based on central-differencing (CD), averaged CD (ACD), and averaged-forward-backward-differencing (AFB), which is equivalent to “rotated scheme” (R) of Willot [229]. Displayed for comparison as well are direct Fourier (F; no finite-difference discretization) and standard finite-element (SFE) solutions at the same resolution [95]

operator which approximates the differential operator in Eq. (9) with first-order finite difference approximations [9, 113, 229, 230] as introduced by Willot [230]. Investigations by [183] show the equivalence of this modified scheme to a FFT-based finite element discretization which includes linear hexahedral elements with reduced integration. The modified FFT-based scheme may be further improved by using a finite difference discretization on a staggered grid, as shown in [182]. In addition, the artificial oscillations may also be treated by using higher-order finite difference approximations as shown in [211, 212].

Other strategies of smoothing the results around discontinuities are based on regularization strategies [3] or composite voxels [93].

In Khorrami et al. [95], spectral algorithms are developed and compared for the numerical solution of periodic (quasi-static) elastic mechanical boundary-value problems. To this end, they employ two different approximations / discretizations of (truncated) Fourier series for periodic fields: (i)

piecewise-constant approximation of the integrand of the Fourier mode integral, and (ii) trapezoidal approximation of this integral. Given these, a number of algorithms are formulated in the context of (I) Green-function preconditioning of stress divergence, and (II) finite-difference discretization of differential operators (i.e., the basis of the so-called “accelerated schemes”: e.g., Moulinec and Silva [154]). These algorithms solve for displacement (i.e., rather than strain: e.g., Moulinec and Suquet [155]; Suquet [197]; Moulinec and Silva [154]; Willot [229]) via iteration (e.g., fixed-point in the linear, or Newton-Krylov in the non-linear, case). Differential operator discretization is based for example on central-differencing (CD), averaged CD (ACD), and averaged-forward-backward-differencing (AFB). As it turns out, AFB is equivalent to the “rotated scheme” (R) of Willot [229] in the context of trapezoidal discretization. Computational comparisons of these and related algorithms are carried out with the help of the (classic) benchmark case of a cubic-inclusion-matrix composite (e.g., Suquet [197]; Willot [229]) with discontinuous phase contrast at the matrix–inclusion interface (Fig. 6). Related algorithms compared include that of Eloh et al. [52] based on the so-called “discrete Green operator”, which employs piecewise-constant discretization, and Green-function preconditioning in Lippmann–Schwinger form, but not finite-difference discretization. For more information, the interested reader is referred to Khorrami et al. [95].

3.4 Model Order Reduction Techniques for FFT-Based Solvers

Even though the FFT-based simulation of heterogeneous microstructures is already an efficient solution scheme, the computational costs for the simulation of highly resolved complex microstructures is still very intensive. Due to that, a recent research topic is the combination of the FFT-based solvers with model order reduction techniques.

A first FFT-based solver incorporating a model order reduction technique is given in [62] based on a proper orthogonal decomposition (POD), [165]. The POD projects the system equations onto a subspace spanned by a reduced basis of ‘small’ dimension. Doing that, so-called ‘snapshots’ need to be generated in a pre-processing step considering for example different loadings and loading directions. Subsequently, a snapshot matrix is computed, containing the corresponding strain solutions $\hat{\epsilon}$ in Fourier space, followed by a singular value decomposition of this matrix and the computation of a projector operator for a given amount of the largest eigenvalues. This leads to a significant reduction of the computational time, with the drawback of a time consuming pre-processing step for the snapshot generation (but which must be only performed once for a given set of parameters).

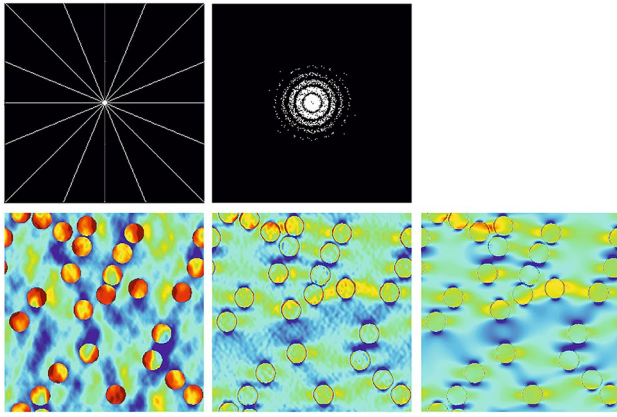


Fig. 7 Fixed radial and geometrically adapted set of Fourier modes (*top*) and corresponding and reference stress distribution in a periodic composite microstructure (*bottom*)

Another model order reduction technique for the FFT-based microstructure simulation adapted to the intrinsic character of the spectral solver is based on solving the Lippmann–Schwinger equation in Fourier space (Eq. 5) by considering only a reduced set of Fourier modes. For this purpose, all Fourier modes are arranged on a grid with the lowest Fourier modes in the center. The first idea was to use a fixed, radial sampling pattern on this grid to determine the reduced set of Fourier modes [104]. After solving the Lippmann–Schwinger equation with this reduced set of Fourier modes, a reconstruction algorithm based on the TV_1 -algorithm [23] and a compatibility step was used to generate highly resolved microstructural fields. Since a fixed sampling pattern is used for all computations, no time consuming pre-processing step is necessary. An extension of this algorithm to finite strain kinematics is given in [68]. The accuracy of this model order reduction technique depends on the one hand on the number of considered Fourier modes and on the other hand on the choice of the considered Fourier modes. Due to that, an improved technique for the generation of a reduced set of wave vectors based on a geometrically adapted sampling pattern is proposed in [70]. Considering the same amount of Fourier modes, the solution based on such an adapted reduced set of Fourier modes leads to more accurate microstructural fields even without the reconstruction and compatibility step is given in Fig. 7. In [70] also a three dimensional extension of this model order reduction technique is given.

Yet another model order reduction technique is proposed in [220] based on low-rank tensor approximations. Within low-rank approximations, tensors are expressed by a smaller set of parameters (e.g. the representation of a second order tensor in terms of a generalized singular

value) [140]. The utilization and investigation of different low-rank tensor approximations in terms of the Fourier–Galerkin method [218] again leads to an efficient FFT-based method.

3.5 Application of FFT-Based Simulations

The FFT-based simulation approach was introduced first in the context of computing the micromechanical fields within periodic microstructures of composite materials [155, 156]. The utilization of this method in terms of polycrystalline microstructures is given in [112]. In the past, numerous investigations and improvements for these simulations followed. An overview of microscale simulations of composites or polycrystalline materials in terms of the FFT-based simulation is presented in Sects. 3.5.1 and 3.5.2, respectively.

3.5.1 FFT-Based Simulation of Composite Microstructures

Considering linear or nonlinear mechanical composites with finite phase contrast, such as fiber reinforced materials, the FFT-based method was introduced in [155, 156] as alternative to the common FE-based microstructure simulation. Using the FFT-based method spatially resolved microstructural fields such as the microstructural strain field in a glass fiber reinforced plastic microstructure may be computed, see Fig. 8.

To model composites with infinite phase contrast, such as microstructures with voids or rigid inclusions, an extension of the basic fixed-point scheme based on augmented Lagrangians was introduced in [145]. This method is applied in [14, 15] to investigate the effect of the microstructural distribution of voids in composite materials on the plastic overall response. In [89] also a comparison of similar results with the results from analytical homogenization is given. In addition, the effective properties of two-phase composites reinforced by randomly distributed spherical particles are investigated and compared to analytical homogenization methods in [66]. Both studies showed that the analytical models do not provide accurate results for a wide range of phase contrasts and volume fractions. Furthermore, in [128] the FFT-based method is used to predict the material properties in additively manufactured structures and in [32] to display the mechanical fields in thermoplastic polymer composites filled with hollow glass microspheres. Also the effective properties of sheet molding compound composites may be computed in terms of a FFT-based simulation [74].

Besides the investigation on classical composites, the FFT-based method was also used to investigate the behavior of calcium silicate hydrates (C-S-H) in hardened cement paste [193]. The influence of size, distribution and shape of inclusions on the concrete creep properties was shown in [111] and the effect of regular and irregular coarse

aggregates in self-compacting high-performance concrete was investigated in [162].

An additional field of the mechanical microstructure simulation is the prediction of the micromechanical damage behavior. In [196] the FFT-based method is combined with continuum damage mechanics to model the failure and progressive damage in composite materials. A similar simulation approach is used to compute the stiffness and strength of medium density fiberboards [192], to capture the progressive damage in 3D braided composites [222] and to capture the damage evolution in porous media, such as sandstone [126]. Instead of the continuum damage approach, the FFT-based method may also be combined with a phase-field approach [2, 22] to model the damage evolution. This approach was used to investigate the brittle fracture in an idealized continuous fiber composite [35, 53] and to analyze the damage initiation in a Silicon carbide (SiC/SiC) composite tube [34].

The FFT-based method furthermore enables to compute the microscopic responses of composite microstructures in different, non-mechanical contexts. This is for example necessary to investigate the behavior of thermoelastic composites [213], the thermal properties of liquid metal elastomeric composites [39], the electrical conduction in periodic composites [230, 233], the electro-mechanically coupled material behavior [73] or the elastic wave propagation in heterogeneous media [26].

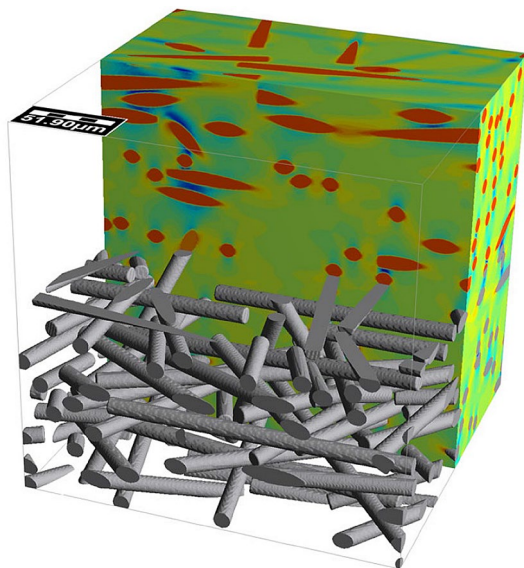


Fig. 8 Strain distribution in a periodic glass fiber reinforced plastic microstructure [92]

3.5.2 FFT-Based Simulation of Polycrystalline Microstructures

A general overview describing anisotropic heterogeneous crystalline materials is given in [173], discussing constitutive laws, kinematics, multiscale techniques and comparisons to experimental results. Considering computational homogenization of polycrystalline microstructures a detailed review is given in [188]. Lebensohn [112] was the first to utilize the FFT-based method in this context incorporating a rigid-viscoplastic material behavior. This full-field simulation approach was for example used to validate analytical methods for the prediction of the effective microstructural response in [3, 18, 117].

To generate polycrystalline microstructures, one possibility is to use a Voronoi tessellation as shown in [6, 7, 40]. An advantage of the FFT-based method is the possibility of computing the microstructural fields directly from an image of their microstructure. Therefore, modelling the subgrain texture evolution directly based on polycrystalline microstructures from electron back-scattering diffraction (EBSD)-based orientation imaging microscopy (OIM) was proposed in [118]. Using such polycrystalline microstructures, numerical experiments have been performed to show for example that stress hot spots occur close to grain boundaries [171]. In addition, the influence of the volume fraction and the contiguity of isotropic particles embedded in a polycrystalline matrix phase on the stress and strain-rate fields is investigated in [114]. It showed that the first and second moments of the stress and strain-rate are differently affected by these properties.

A generalization of the rigid-viscoplastic material behavior to an elasto-viscoplastic formulation in terms of a FFT-based microstructure simulation (EVP-FFT) is given by Lebensohn et al. [122] considering the small strain regime and by Eisenlohr et al. [49] considering the finite strain regime. Using this EVP-FFT-based method, further studies modelled the internal lattice strain distributions in stainless steel [94] or in dual phase steel microstructures [24, 41, 163]. Some exemplary results of using this EVP-FFT model are shown in Fig. 9. A modification to include the shear transformation strain associated with deformation twinning is presented in [108, 109, 160]. Another extension of this model is based on augmented Lagrangians [145] for the simulation of void growth in polycrystalline materials [123]. This modified simulation approach is used to investigate the mechanical behavior of metal additive manufactured microstructures [36]. It showed that pores, which result from the additive manufacturing process itself, lead to significant stress hotspots.

Coupling the EVP-FFT-based method with a phase-field model [2, 22] enables the simulation of different additional physical processes. Examples are simulations to capture the recrystallization of polycrystals [33, 236],

phase transformations [100] and fracture within polycrystalline microstructures [135], respectively. Further extensions concern the modelling of fatigue crack growth [175, 176], modelling interface decohesion in terms of a nonlocal interphase [190] or a gradient damage approach [191]. Incorporating crystallographic defects in terms of dislocations, introduced in [215], the EVP-FFT-based method was coupled with field dislocation dynamics (FDM) in [9, 10, 42] and discrete dislocation dynamics in [11, 12, 178]. To investigate the grain size on the flow stress of polycrystals, known as the Hall-Petch effect [77, 164], also an intrinsic material length scale associated with the plastic strain gradients may be introduced resulting in a strain gradient crystal plasticity approach [79, 113].

A comparison of the computed micromechanical fields to experimental mechanical fields is given in [166, 201, 202], with the microstructure model directly gained from EBSD measurements. The study confirmed a good correlation between the averaged results obtained from experiments and the results from simulations, while the local microstructural results do agree qualitatively. In addition, a virtual laboratory approach is introduced in [235] to determine the initial yield surface for sheet metal forming operations based on highly resolved microstructural FFT-based simulations and to compare the results to experimental investigations.

An earlier overview of FFT-based simulation of polycrystalline microstructures is given in [115, 121] and the free simulation software DAMASK for the simulation of polycrystalline microstructures based on finite elements or fast Fourier transforms is introduced in [172, 174].

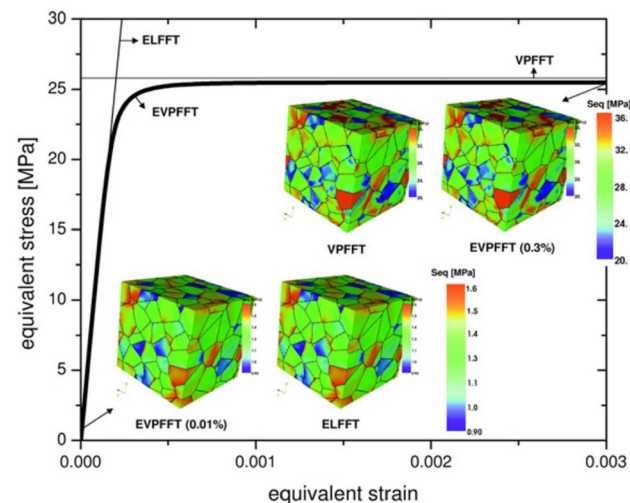


Fig. 9 Effective equivalent stress–strain curve and microstructural equivalent stress fields S_{eq} predicted by the EVP–FFT model. For comparison, the results of a FFT-based simulation of a purely elastic (EL-FFT) and a purely viscoplastic (VP-FFT) material model with the same material parameters are shown [122]

Besides the investigations on polycrystalline metallic microstructures, also the simulation of the micromechanical fields within polycrystalline ice was performed by using a FFT-based method [75, 119, 198].

3.6 Comparison Between FE- and FFT-Based Computational Methods

Compared to finite element simulations one major advantage of FFT-based simulations is the image processing-like character and the associated possibility of directly using images of a real microstructure for the numerical simulation [118, 155, 156]. Therefore, in contrast to the finite element method, it avoids possible difficulties due to meshing of complex microstructures. In addition, several studies [129, 144, 167] showed, that the FFT-based method is more efficient than a classical FE-based microstructure simulation under the condition of periodicity.

A major disadvantage of FFT-based microstructure simulations is the restriction to periodic microstructures. This results from the intrinsic periodic ansatz functions. Nevertheless, considering a multiscale simulation these periodic microstructures are usually desired. In this case no additional effort is needed to prescribe the periodic boundary conditions.

Other disadvantages of the FFT-based basic fixed-point scheme are related to resolution errors due to the Gibbs phenomenon and numerical problems treating composites with high or infinite phase contrasts. These problems were addressed and solved in several works. Solutions concerning the resolution errors are for example elaborated in [3, 93, 211, 229, 230] by using finite difference approximations of the differential operator in Eq. (9) or using composite voxels. Solutions concerning the treatment of microstructures with infinite phase contrast are addressed in [122, 145, 146, 152, 184] using polarization based schemes, solution schemes based on augmented Lagrangians or conjugate gradient solvers.

Based on the Galerkin discretization, introduced in [19, 20, 218] and improved in [216, 219], the analogy of the FFT-based solver to finite element based simulations is finally shown in [38, 179, 234]. This is done by constructing the FFT-based solver using a similar variational basis as for conventional FE methods. Due to that, the constitutive routines of the FE methods may directly be used within the FFT-based framework, while still profiting from the computational efficiency of the FFT-based solver.

4 FE-FFT-Based Two-Scale Simulation

The voxel like character of Fourier spectral solvers results in simple discretization of the underlying microstructure and periodic global ansatz functions intrinsically imply periodic boundary conditions. For this reason, the FFT-based method is a well-suited and efficient solver for the microscopic BVP in terms of a two-scale FE-FFT-based simulation. In this context, the macroscopic BVP is discretized into finite elements while the microscopic BVP is defined by a distinct number of grid points, see Fig. 10. The overall macroscopic material behavior is then defined as volume average of its microscopic counterpart, which yields

$$\bar{\epsilon}(\bar{x}) := \frac{1}{\Omega} \int_{\Omega} \epsilon(\bar{x}, x) d\Omega \tag{10}$$

$$\bar{\sigma}(\bar{x}) := \frac{1}{\Omega} \int_{\Omega} \sigma(\bar{x}, x) d\Omega \tag{11}$$

in terms of small strain kinematics.

The novel FE-FFT-based two-scale simulation approach was first introduced for modeling progressive damage within fiber-reinforced composites in [196]. As a first approach, the latter authors utilized the basic fixed-point scheme [155, 156] for the FFT-based microstructure simulation within a small strain regime. A more efficient FE-FFT-based two-scale method was proposed in [100] based on augmented Lagrangians [122] for the FFT-based simulation of polycrystalline materials incorporating phase-field-based simulations of microstructural phase transformations.

Considering a two-scale simulation, the computation of the macroscopic tangent operator is essential, but computationally very expensive. One way of computing the macroscopic tangent operator is based on a numerical approximation [100, 103, 196]. Therefore, the linearized stress increment

$$\Delta\bar{\sigma} = \frac{\partial\bar{\sigma}}{\partial\bar{\epsilon}} : \Delta\bar{\epsilon} \tag{12}$$

and the perturbed strain field

$$\bar{\epsilon}_\Delta^{kl} = \bar{\epsilon} + \frac{\Delta\bar{\epsilon}}{2} (\mathbf{e}_k \otimes \mathbf{e}_l + \mathbf{e}_l \otimes \mathbf{e}_k) = \bar{\epsilon} + \Delta\bar{\epsilon}^{kl} \tag{13}$$

with the perturbation strain $\Delta\bar{\epsilon}$ need to be taken into account. Performing a forward difference approximation of the stress increment and considering the definition of the perturbed strain field, the numerical tangent operator yields

$$\bar{\mathbb{C}}_{ijkl} = \frac{\partial\bar{\sigma}_{ij}}{\partial\bar{\epsilon}_{kl}} \approx \frac{\bar{\sigma}_{ij}(\bar{\epsilon}_\Delta^{kl}) - \bar{\sigma}_{ij}(\bar{\epsilon})}{\Delta\bar{\epsilon}}. \tag{14}$$

Consequently, in the three-dimensional case, six perturbations are necessary to compute the numerical tangent

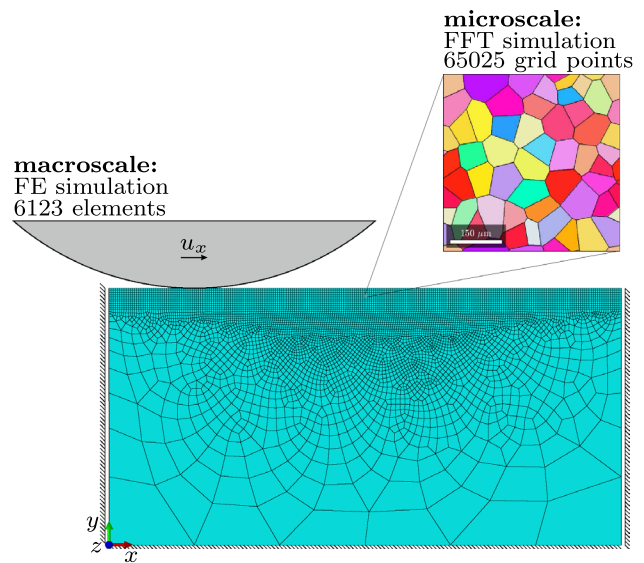


Fig. 10 Example of a two-scale FE-FFT-based simulation. The FE simulation is used on the macroscale, while the FFT-based simulation is used on the periodic microscale

operator. These perturbation must be as small as possible in order to obtain an accurate approximation of the analytical tangent operator, while numerical problems due to too small perturbations need to be avoided, which leads to values between $\Delta\bar{\epsilon} = 10^{-8}$ and $\Delta\bar{\epsilon} = 10^{-6}$ for the perturbation.

Considering finite strain kinematics, with the macroscopic first Piola–Kirchhoff stress tensor $\bar{\mathbf{P}}$ and the macroscopic deformation gradient $\bar{\mathbf{F}}$, nine perturbations are needed in general to compute the numerical tangent operator, since $\bar{\mathbf{F}}$ is not symmetric. An efficient method based on only six instead of these nine perturbations was proposed in [101, 147].

Another method for the computation of the macroscopic tangent operator is derived by means of the Lippmann–Schwinger equation and can be computed from a system of linear equations, as shown in [72]. To deduce the aforementioned system of linear equations, the linearized stress increment (12) is transformed into

$$\Delta\bar{\sigma} = \frac{1}{\Omega} \left[\int_{\Omega} \mathbb{C} d\Omega + \int_{\Omega} \mathbb{C} : \frac{\partial\bar{\epsilon}}{\partial\bar{\epsilon}} d\Omega \right] : \Delta\bar{\epsilon} \tag{15}$$

as shown in [149, 150]. This leads to the definition of the algorithmically consistent macroscopic tangent

$$\mathbb{C}^{\text{algo}} := \frac{1}{\Omega} \left[\int_{\Omega} \mathbb{C} d\Omega + \int_{\Omega} \mathbb{C} : \frac{\partial\bar{\epsilon}}{\partial\bar{\epsilon}} d\Omega \right]. \tag{16}$$

Within this definition, the first part of the equation

$$\bar{\mathbb{C}}^V = \frac{1}{\Omega} \int_{\Omega} \mathbb{C} \, d\Omega \quad (17)$$

is the effective stiffness tensor as defined by Voigt [214]. In addition, the derivative of the fluctuation strain field $\tilde{\epsilon}$ with respect to the macroscopic strain field $\bar{\epsilon}$ can be determined by solving the following linear equation system:

$$\mathbb{F}^0 * [\mathbb{C} - \mathbb{C}^0] = \mathbb{F}^0 * \left[(\mathbb{C} - \mathbb{C}^0) : \frac{\partial \tilde{\epsilon}}{\partial \bar{\epsilon}} \right] - \frac{\partial \tilde{\epsilon}}{\partial \bar{\epsilon}}. \quad (18)$$

A straight forward extension of this definition of the algorithmically consistent macroscopic tangent operator to finite strains is given in [72] and leads to a speedup of 1.5 to 2 for different material behaviors compared to the aforementioned numerical tangent operator.

Since a two-scale full field simulation is computationally expensive, an efficient and accurate FE-FFT-based simulation procedure was proposed in [102, 103], while the FFT-based microstructure simulation is based on a Newton-Krylov solution scheme [64, 92, 233]. The efficient solution procedure is based on a pre-processing, a processing and a post-processing step. Within the pre-processing step different discretizations of a polycrystalline microstructure with different textures, number of grains and prescribed macroscopic strains are investigated. This leads to a minimal number of grid points, which is necessary to obtain an accurate macroscopic response. The resulting coarsely discretized microstructure is utilized within the actual two-scale simulation, while the history of the macroscopic strain of any point of particular interest is saved. Finally, in the post-processing step, this macroscopic strain and a finely discretized microstructure are used to generate highly resolved microstructural fields for these macroscopic points, see Fig. 11. A generalization of this simulation procedure to finite strain kinematics is given in [69].

Another efficient simulation strategy is based on using highly resolved full field simulations only in macroscopic critical areas. In this context, an algorithm, which uses a database with certain tangent operators for the macroscopic simulation of fiberboards and switches to a full field FE-FFT-based two scale simulation if no appropriate tangent operator is available, was proposed in [192]. A similar approach is presented in [98, 224], in which a FFT-based simulation is used to train a database model in a pre-processing step. Within the actual two-scale FE-FFT-based simulation, this database model is used in general, except for macroscopic critical areas, in which a highly resolved full field simulation is performed to capture the viscoelastic and fatigue behavior of short fiber-reinforced polymers.

In contrast to the aforementioned fully coupled concurrent FE-FFT-based simulation approaches, a solution strategy based on an exclusively macroscopic FE simulation followed by an FFT-based simulation of distinct macroscopic

integration points was applied in [206]. Doing that, a quantitative understanding of the load dependence of lattice strain evolution during monotonic loading was obtained. In addition, the intergranular strain evolution during biaxial loading [207] and the role of microstructural evolution, such as texture, anisotropy and dislocation density was investigated [208] in a similar manner. Finally, this two-scale simulation approach was used to predict and explain the lattice strain and intensity evolution of microstructures gained from in-situ diffraction experiments [209].

In the following, some more applications of the FE-FFT-based multiscale approach are listed. The utilization of the two-scale simulation approach to magneto-mechanically and electro-mechanically coupled materials at finite strains is given in [168] and [73], respectively. In addition, the FE-FFT-based method was used to investigate the process-structure-property relationship for additive manufacturing in a small strain regime in [132]. The application of the software DAMASK [172, 174] within a multiscale framework has recently been presented in [78]. Finally, investigating braided composite beams in terms of a FE-FFT-based two-scale simulation [57, 223], the FFT-based microstructure simulation based on variational methods [38, 216, 222] was used within the two-scale context, to overcome the poor convergence behavior of FFT-based solvers in terms of composites with high phase contrasts.

An overview of the FE-FFT-based algorithms and their applications is also given in Table 3.

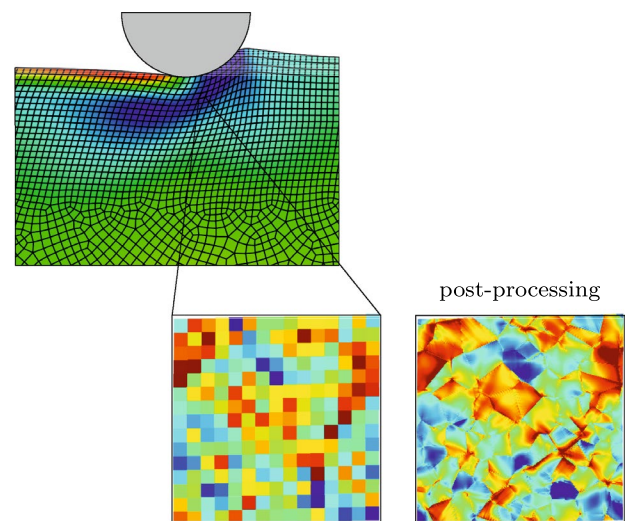


Fig. 11 Efficient FE-FFT-based two-scale simulation with a coarse discretized microstructure, followed by a post-processing step to generate highly resolved microstructural data

Table 3 FE-FFT-based algorithms and applications

Algorithms and applications	Key references
Concurrent FE-FFT-based simulation	Spahn et al. [196], Sliseris et al. [192], Kochmann et al. [100–103], Göküzüm and Keip [72], Rambausek et al. [168], Göküzüm et al. [73], Welschinger et al. [224], Fang et al. [57], Wang et al. [223], Han et al. [78], Köbler et al. [98], Gierden et al. [69]
Non-concurrent FE-FFT-based simulation	Upadhyay et al. [206–209], Liu et al. [132]
Macroscopic tangent operator	
Numerical tangent operator	Spahn et al. [196], Sliseris et al. [192], Kochmann et al. [100–103], Fang et al. [57], Wang et al. [223], Gierden et al. [69]
Algorithmically consistent tangent operator	Göküzüm and Keip [72], Rambausek et al. [168], Göküzüm et al. [73]
Incorporating MOR techniques	Sliseris et al. [192], Kochmann et al. [102, 103], Welschinger et al. [224], Köbler et al. [98], Gierden et al. [69]
Simulation of composite microstructures	Spahn et al. [196], Göküzüm and Keip [72], Rambausek et al. [168], Göküzüm et al. [73], Welschinger et al. [224], Fang et al. [57], Wang et al. [223], Köbler et al. [98]
Simulation of polycrystalline microstructures	Kochmann et al. [100], Upadhyay et al. [207–209], Kochmann et al. [101–103], Liu et al. [132], Han et al. [78], Gierden et al. [69]

5 Conclusion

For periodic micro-heterogeneous materials, the FFT-based method represents a computational method which is a suitable alternative to classical FE-based methods. In the last two and a half decades this FFT-based method has proven to be a fast and accurate tool in regard of a computational microscale simulation. One major advantage of FFT-based simulations compared to FE-based simulations is the image processing-like character and, connected to that, the possibility to directly employ images of a real microstructure for the numerical simulation. This avoids the meshing of complex microstructures.

Possible problems of the FFT-based method concern the convergence behavior within simulations of microstructures incorporating infinite phase contrasts and artificial oscillations around discontinuities related to the Gibbs phenomenon. These problems were solved by developing accelerated solution methods (e.g. polarization based methods, methods based on augmented Lagrangians, gradient decent methods, or quasi-Newton methods) and using for example finite difference approximations of the Lippmann–Schwinger, composite voxels or a discrete Greens operator, respectively. This leads to a solution scheme, which is even more efficient than the classical FE-based microstructure simulation. Nevertheless, the FFT-based microstructure simulation is exclusively restricted to investigations on periodic microstructures, while there are no further restrictions for the FE-based microstructure simulation.

To generate an even more efficient simulation approach model order reduction techniques for FFT-based solvers were developed recently. These progresses and the intrinsic periodic character of the spectral solver including intrinsic periodic boundary conditions, lead to a well-suited scheme

in terms of an efficient and accurate FE-FFT-based two-scale method.

Acknowledgements The authors gratefully acknowledge the financial support of the research work by the German Research Foundation (DFG, Deutsche Forschungsgemeinschaft) within the trans-regional Collaborative Research Center SFB/TRR 136, Project Number 223500200, subprojects M03 and M05. Additionally, we thank Mohammad Khorrami for many helpful discussions.

Funding Open Access funding enabled and organized by Projekt DEAL.

Declarations

Conflict of interest The authors declare that they have no conflict of interest.

Open Access This article is licensed under a Creative Commons Attribution 4.0 International License, which permits use, sharing, adaptation, distribution and reproduction in any medium or format, as long as you give appropriate credit to the original author(s) and the source, provide a link to the Creative Commons licence, and indicate if changes were made. The images or other third party material in this article are included in the article's Creative Commons licence, unless indicated otherwise in a credit line to the material. If material is not included in the article's Creative Commons licence and your intended use is not permitted by statutory regulation or exceeds the permitted use, you will need to obtain permission directly from the copyright holder. To view a copy of this licence, visit <http://creativecommons.org/licenses/by/4.0/>.

References

1. Abdulle A, Weinan E (2003) Finite difference heterogeneous multi-scale method for homogenization problems. *J Comput Phys* 191(1):18–39
2. Allen SM, Cahn JW (1979) A microscopic theory for antiphase boundary motion and its application to antiphase domain coarsening. *Acta Metall* 27(6):1085–1095

3. Anglin BS, Lebensohn RA, Rollett AD (2014) Validation of a numerical method based on Fast Fourier Transforms for heterogeneous thermoelastic materials by comparison with analytical solutions. *Comput Mater Sci* 87:209–217
4. Artioli E, Marfia S, Sacco E (2018) High-order virtual element method for the homogenization of long fiber nonlinear composites. *Comput Methods Appl Mech Eng* 341:571–585
5. Balzani D, Brands D, Schröder J, Carstensen C (2010) Sensitivity analysis of statistical measures for the reconstruction of microstructures based on the minimization of generalized least-square functionals. *Tech Mech* 30(4):297–315
6. Barbe F, Decker L, Jeulin D, Cailletaud G (2001) Intergranular and intragranular behavior of polycrystalline aggregates. Part 1: F.E. model. *Int J Plasticity* 17(4):513–536
7. Barbe F, Decker L, Jeulin D, Cailletaud G (2001) Intergranular and intragranular behavior of polycrystalline aggregates. Part 2: results. *Int J Plasticity* 17(4):537–563
8. Belytschko T, Liu WK, Moran B (2000) *Nonlinear finite elements for continua and structures*. Wiley, Chichester
9. Berbenni S, Taupin V, Djaka KS, Fressengeas C (2014) A numerical spectral approach for solving elasto-static field dislocation and g-disclination mechanics. *Int J Solids Struct* 51(23–24):4157–4175
10. Berbenni S, Taupin V, Lebensohn RA (2020) A fast Fourier transform-based mesoscale field dislocation mechanics study of grain size effects and reversible plasticity in polycrystals. *J Mech Phys Solids* 135:103808
11. Bertin N, Capolungo L (2018) A FFT-based formulation for discrete dislocation dynamics in heterogeneous media. *J Comput Phys* 355:366–384
12. Bertin N, Upadhyay MV, Pradalier C, Capolungo L (2015) A FFT-based formulation for efficient mechanical fields computation in isotropic and anisotropic periodic discrete dislocation dynamics. *Model Simul Mater Sci Eng* 23:065009
13. Bhattacharya K, Suquet PM (2005) A model problem concerning recoverable strains of shape-memory polycrystals. *Proc R Soc Lond Ser A Math Phys Eng Sci* 461:2797–2816
14. Bilger N, Auslender F, Bornert M, Michel JC, Moulinec H, Suquet P, Zaoui A (2005) Effect of a nonuniform distribution of voids on the plastic response of voided materials: a computational and statistical analysis. *Int J Solids Struct* 42:517–538
15. Bilger N, Auslender F, Bornert M, Moulinec H, Zaoui A (2007) Bounds and estimates for the effective yield surface of porous media with a uniform or a nonuniform distribution of voids. *Eur J Mech A Solids* 26(5):810–836
16. Boeff M, Gutknecht F, Engels PS, Ma A, Hartmaier A (2015) Formulation of nonlocal damage models based on spectral methods for application to complex microstructures. *Eng Fract Mech* 147:373–387
17. Bonnet G (2007) Effective properties of elastic periodic composites with fibers. *J Mech Phys Solids* 55(5):881–899
18. Brenner R, Lebensohn RA, Castelnau O (2009) Elastic anisotropy and yield surface estimates of polycrystals. *Int J Solids Struct* 46(16):3018–3026
19. Brisard S, Dormieux L (2010) FFT-based methods for the mechanics of composites: a general variational framework. *Comput Mater Sci* 49(3):663–671
20. Brisard S, Dormieux L (2012) Combining Galerkin approximation techniques with the principle of Hashin and Shtrikman to derive a new FFT-based numerical method for the homogenization of composites. *Comput Methods Appl Mech Eng* 217–220:197–212
21. Budiansky B (1965) On the elastic moduli of some heterogeneous materials. *J Mech Phys Solids* 13(4):223–227
22. Cahn JW, Hilliard JE (1958) Free energy of a nonuniform system. I. Interfacial free energy. *J Chem Phys* 28:258–267
23. Candes EJ, Romberg J, Tao T (2006) Robust uncertainty principles: exact signal reconstruction from highly incomplete frequency information. *IEEE Trans Inf Theory* 52(2):489–509
24. Cantara AM, Zecevic M, Eghtesad A, Poulin CM, Knezevic M (2019) Predicting elastic anisotropy of dual-phase steels based on crystal mechanics and microstructure. *Int J Mech Sci* 151:639–649
25. Cao YJ, Shen WQ, Shao JF, Wang W (2020) A novel FFT-based phase field model for damage and cracking behavior of heterogeneous materials. *Int J Plasticity* 133:102786
26. Capdeville Y, Zhao M, Cupillard P (2015) Fast Fourier homogenization for elastic wave propagation in complex media. *Wave Motion* 54:170–186
27. Castañeda PP (1996) Exact second-order estimates for the effective mechanical properties of nonlinear composites. *J Mech Phys Solids* 44(6):827–862
28. Castañeda PP (2002) Second-order homogenization estimates for nonlinear composites incorporating field fluctuations. I—theory. *J Mech Phys Solids* 50(4):737–757
29. Castañeda PP (2002) Second-order homogenization estimates for nonlinear composites incorporating field fluctuations. II—applications. *J Mech Phys Solids* 50(4):759–782
30. Castañeda PP, Suquet P (1997) Nonlinear composites. *Adv Appl Mech* 34:171–302
31. Cavaliere F, Wulfinghoff S, Reese S (2020) Efficient two-scale simulations of engineering structures using the Hashin–Shtrikman type finite element method. *Comput Mech* 65:159–175
32. Charière R, Marano A, Gélébart L (2020) Use of composite voxels in FFT based elastic simulations of hollow glass microspheres/polypropylene composites. *Int J Solids Struct* 182–183:1–14
33. Chen L, Chen J, Lebensohn RA, Ji YZ, Heo TW, Bhattacharyya S, Chang K, Mathaudhu S, Liu ZK, Chen LQ (2015) An integrated fast Fourier transform-based phase-field and crystal plasticity approach to model recrystallization of three dimensional polycrystals. *Comput Methods Appl Mech Eng* 285:829–848
34. Chen Y, Gélébart L, Chateau C, Bornert M, Sauder C, King A (2019) Analysis of the damage initiation in a SiC/SiC composite tube from a direct comparison between large-scale numerical simulation and synchrotron X-ray micro-computed tomography. *Int J Solids Struct* 161:111–126
35. Chen Y, Vasiukov D, Gélébart L, Park CH (2019) A FFT solver for variational phase-field modeling of brittle fracture. *Comput Methods Appl Mech Eng* 349:167–190
36. Cunningham R, Nicolas A, Madsen J, Fodran E, Agnostou E, Sangid MD, Rollett AD (2017) Analyzing the effects of powder and post-processing on porosity and properties of electron beam melted Ti-6Al-4V. *Mater Res Lett* 5(7):516–525
37. deBotton G, Castañeda PP (1995) Variational estimates for the creep behaviour of polycrystals. *Proc R Soc A Math Phys Eng Sci* 448:121–142
38. de Geus TWJ, Vondřejc J, Zeman J, Peerlings RHJ, Geers MGD (2017) Finite strain FFT-based non-linear solvers made simple. *Comput Methods Appl Mech Eng* 318:412–430
39. Dehnavi FN, Safdari M, Abrinia K, Sheidaei A, Baniassadi M (2020) Numerical study of the conductive liquid metal elastomeric composites. *Mater Today Commun* 23:100878
40. Diard O, Leclercq S, Rousselier G, Cailletaud G (2005) Evaluation of finite element based analysis of 3D multicrystalline aggregates plasticity—application to crystal plasticity model identification and the study of stress and strain fields near grain boundaries. *Int J Plasticity* 21(4):691–722
41. Diehl M, An D, Shanthraj P, Zaefferer S, Roters F, Raabe D (2017) Crystal plasticity study on stress and strain partitioning in a measured 3D dual phase steel microstructure. *Phys Mesomech* 20:311–323

42. Djaka KS, Berbenni S, Taupin V, Lebensohn RA (2020) A FFT-based numerical implementation of mesoscale field dislocation mechanics: application to two-phase laminates. *Int J Solids Struct* 184:136–152
43. Dreyer W, Müller WH (2000) A study of the coarsening of tin/lead solders. *Int J Solids Struct* 37(28):3841–3871
44. Drugan WJ, Willis JR (1996) A micromechanics-based nonlocal constitutive equation and estimates of representative volume element size for elastic composites. *J Mech Phys Solids* 44(4):497–524
45. Dvorak GJ (1992) Transformation field analysis of inelastic composite materials. *Proc R Soc A Math Phys Eng Sci* 437(1900):311–327
46. Eghesad A, Barrett TJ, Germaschewski K, Lebensohn RA, McCabe RJ, Knezevic M (2018) OpenMP and MPI implementations of an elasto-viscoplastic fast Fourier transform-based micromechanical solver for fast crystal plasticity modeling. *Adv Eng Softw* 126:46–60
47. Eghesad A, Germaschewski K, Lebensohn RA, Knezevic M (2020) A multi-GPU implementation of a full-field crystal plasticity solver for efficient modeling of high-resolution microstructures. *Comput Phys Commun* 254:107231
48. Eghesad A, Knezevic M (2020) High-performance full-field crystal plasticity with dislocation-based hardening and slip system back-stress laws: Application to modeling deformation of dual-phase steels. *J Mech Phys Solids* 134:103750
49. Eisenlohr P, Diehl M, Lebensohn RA, Roters F (2013) A spectral method solution to crystal elasto-viscoplasticity at finite strains. *Int J Plasticity* 46:37–53
50. El Shawish S, Vincent PG, Moulinec H, Cizelj L, Gélébart L (2020) Full-field polycrystal plasticity simulations of neutron-irradiated austenitic stainless steel: A comparison between FE and FFT-based approaches. *J Nucl Mater* 529:151927
51. Eloh KS, Jacques A, Ribarik G, Berbenni S (2018) The effect of crystal defects on 3D high-resolution diffraction peaks: a FFT-based method. *Materials* 11(9):1669
52. Eloh KS, Jacques A, Berbenni S (2019) Development of a new consistent discrete green operator for FFT-based methods to solve heterogeneous problems with eigenstrains. *Int J Plasticity* 116:1–23
53. Ernesti F, Schneider M, Böhlke T (2020) Fast implicit solvers for phase-field fracture problems on heterogeneous microstructures. *Comput Methods Appl Mech Eng* 363:112793
54. Eshelby JD (1957) The determination of the elastic field of an ellipsoidal inclusion, and related problems. *Proc R Soc A Math Phys Eng Sci* 241(1126):376–396
55. Exner HE, Hougardy HP (1986) Einführung in die quantitative Gefügeanalyse. Deutsche Gesellschaft für Metallkunde
56. Eyre DJ, Milton GW (1999) A fast numerical scheme for computing the response of composites using grid refinement. *Eur Phys J Appl Phys* 6(1):41–47
57. Fang G, Wang B, Liang J (2019) A coupled FE-FFT multiscale method for progressive damage analysis of 3D braided composite beam under bending load. *Compos Sci Technol* 181:107691
58. Feyel F, Chaboche JL (2000) FES²S multiscale approach for modeling the elastoviscoplastic behaviour of long fibre SiC/Ti composite materials. *Comput Methods Appl Mech Eng* 183(2–3):309–330
59. Fish J, Shek K, Pandheeradi M, Shephard MS (1997) Computational plasticity for composite structures based on mathematical homogenization: theory and practice. *Comput Methods Appl Mech Eng* 148(1–2):53–73
60. Fritzen F, Böhlke T (2010) Three-dimensional finite element implementation of the nonuniform transformation field analysis. *Int J Numer Methods Eng* 84(7):823–849
61. Fritzen F, Leuschner M (2013) Reduced basis hybrid computational homogenization based on a mixed incremental formulation. *Comput Methods Appl Mech Eng* 260:143–154
62. Garcia-Cardona C, Lebensohn R, Anghel M (2017) Parameter estimation in a thermoelastic composite problem via adjoint formulation and model reduction. *Int J Numer Methods Eng* 112(6):578–600
63. Geers MGD, Kouznetsova VG, Brekelmans WAM (2010) Multi-scale computational homogenization: trends and challenges. *J Comput Appl Math* 234(7):2175–2182
64. Gélébart L, Mondon-Cancel R (2013) Non-linear extension of FFT-based methods accelerated by conjugate gradients to evaluate the mechanical behavior of composite materials. *Comput Mater Sci* 77:430–439
65. Ghosh S, Lee K, Moorthy S (1995) Multiple scale analysis of heterogeneous elastic structures using homogenization theory and voronoi cell finite element method. *Comput Methods Appl Mech Eng* 32(1):27–62
66. Ghossein E, Lévesque M (2012) A fully automated numerical tool for a comprehensive validation of homogenization models and its application to spherical particles reinforced composites. *Int J Solids Struct* 49(11–12):1387–1398
67. Gibbs JW (1898) Fourier's series. *Nature* 59:200
68. Gierden C, Kochmann J, Manjunatha K, Waimann J, Wulfinghoff S, Svendsen B, Reese S (2019) A model order reduction method for finite strain FFT solvers using a compressed sensing technique. *Proc Appl Math Mech*. 19(1):e201900037.
69. Gierden C, Kochmann J, Waimann J, Kinner-Becker T, Sölter J, Svendsen B, Reese S (2021) Efficient two-scale FE-FFT-based mechanical process simulation of elasto-viscoplastic polycrystals at finite strains. *Comput Methods Appl Mech Eng* 374:113566
70. Gierden C, Waimann J, Svendsen B, Reese S (2021) A model order reduction method for FFT-based microstructure simulation using a geometrically adapted reduced set of frequencies. *Comput Methods Appl Mech Eng* 386:114131
71. Gierden C, Waimann J, Svendsen B, Reese S (2021) FFT-based simulation using a reduced set of frequencies adapted to the underlying microstructure. *Comput Methods Mater Sci* 21(1):51–58
72. Göküzüm FS, Keip MA (2018) An algorithmically consistent macroscopic tangent operator for FFT-based computational homogenization. *Int J Numer Methods Eng* 113(4):581–600
73. Göküzüm FS, Nguyen LTK, Keip MA (2019) A multiscale FE-FFT framework for electro-active materials at finite strains. *Comput Mech* 64:63–84
74. Görthofer J, Schneider M, Ospald F, Hrymak A, Böhlke T (2020) Computational homogenization of sheet molding compound composites based on high fidelity representative volume elements. *Comput Mater Sci* 174:109456
75. Grennerat F, Montagnat M, Castelnau O, Vacher P, Moulinec H, Suquet P, Duval P (2012) Experimental characterization of the intragranular strain field in columnar ice during transient creep. *Acta Mater* 60(8):3655–3666
76. Grimm-Strele H, Kabel M (2019) Runtime optimization of a memory efficient CG solver for FFT-based homogenization: implementation details and scaling results for linear elasticity. *Comput Mech* 64:1339–1345
77. Hall EO (1951) The deformation and ageing of mild steel: III. Discussion of results. *Proc Phys Soc Sect B* 64(9):747–753
78. Han F, Roters F, Raabe D (2020) Microstructure-based multi-scale modeling of large strain plastic deformation by coupling a full-field crystal plasticity-spectral solver with an implicit finite element solver. *Int J Plasticity* 125:97–117
79. Haouala S, Lucarini S, LLorca J, Segurado J (2020) Simulation of the Hall–Petch effect in FCC polycrystals by means of strain

- gradient crystal plasticity and FFT homogenization. *J Mech Phys Solids* 134:103755
80. Hashin Z (1983) Analysis of composite materials—a survey. *J Appl Mech* 50(3):481–505
 81. Hashin Z, Shtrikman S (1962) A variational approach to the theory of the elastic behaviour of polycrystals. *J Mech Phys Solids* 11(2):343–352
 82. Hashin Z, Shtrikman S (1962) On some variational principles in anisotropic and nonhomogeneous elasticity. *J Mech Phys Solids* 10(4):335–342
 83. Hashin Z, Shtrikman S (1963) A variational approach to the theory of the elastic behavior of multiphase materials. *J Mech Phys Solids* 11:127–140
 84. Hershey AV (1954) The elasticity of an isotropic aggregate of anisotropic cubic crystals. *J Appl Mech* 21:236–240
 85. Hill R (1963) Elastic properties of reinforced solids: Some theoretical principles. *J Mech Phys Solids* 11(5):357–372
 86. Hill R (1965) A self-consistent mechanics of composite materials. *J Mech Phys Solids* 13(4):213–222
 87. Hutchinson JW (1976) Bounds and self-consistent estimates for creep of polycrystalline materials. *Proc R Soc A Math Phys Eng Sci* 348(1652):101–127
 88. Idiart MI, Moulinec H, Castañeda PP, Suquet P (2006) Macroscopic behavior and field fluctuations in viscoplastic composites: Second-order estimates versus full-field simulations. *J Mech Phys Solids* 54(5):1029–1063
 89. Idiart MI, Willot F, Pellegrini YP, Castañeda PP (2009) Infinite-contrast periodic composites with strongly nonlinear behavior: effective-medium theory versus full-field simulations. *Int J Solids Struct* 46(18–19):3365–3382
 90. Jacques A (2016) From modeling of plasticity in single-crystal superalloys to high-resolution X-rays three-crystal diffractometer peaks simulation. *Metall Mater Trans A* 47(12):5783–5797
 91. Jaworek D, Waimann J, Gierden C, Wulfinghoff S, Reese S (2020) A Hashin–Shtrikman type semi-analytical homogenization procedure in multiscale modeling to account for coupled problems. *Tech Mech* 40(1):46–52
 92. Kabel M, Böhlke T, Schneider M (2014) Efficient fixed point and Newton–Krylov solvers for FFT-based homogenization of elasticity at large deformations. *Computational Mechanics* 54:1497–1514
 93. Kabel M, Merkert D, Schneider M (2015) Use of composite voxels in FFT-based homogenization. *Comput Methods Appl Mech Eng* 294:168–188
 94. Kanjarla AK, Lebensohn RA, Balogh L, Tomé CN (2012) Study of internal lattice strain distributions in stainless steel using a full-field elasto-viscoplastic formulation based on fast Fourier transforms. *Acta Mater* 60(6–7):3094–3106
 95. Khorrami M, Mianroodi JR, Shanthraj P, Svendsen B (2020) Development and comparison of spectral algorithms for numerical modeling of the quasi-static mechanical behavior of inhomogeneous materials. [arXiv:2009.03762](https://arxiv.org/abs/2009.03762)
 96. Knezevic M, Lebensohn RA, Cazacu O, Revil-Baudard B, Proust G, Vogel SC, Nixon ME (2013) Modeling bending of -titanium with embedded polycrystal plasticity in implicit finite elements. *Mater Sci Eng* 564:116–126
 97. Knezevic M, McCabe RJ, Lebensohn RA, Tomé CN, Liu C, Lovato ML, Mihaila B (2013) Integration of self-consistent polycrystal plasticity with dislocation density based hardening laws within an implicit finite element framework: application to low-symmetry metals. *J Mech Phys Solids* 61(10):2034–2046
 98. Köbler J, Magino N, Andrá H, Welschinger F, Müller R, Schneider M (2021) A computational multi-scale model for the stiffness degradation of short-fiber reinforced plastics subjected to fatigue loading. *Comput Methods Appl Mech Eng* 373:113522
 99. Kochmann J (2019) Efficient FE- and FFT-based two-scale methods for micro-heterogeneous media. Dissertation, Rheinisch-Westfälische Technische Hochschule Aachen
 100. Kochmann J, Wulfinghoff S, Reese S, Mianroodi JR, Svendsen B (2016) Two-scale FE-FFT- and phase-field-based computational modeling of bulk microstructural evolution and macroscopic material behavior. *Comput Methods Appl Mech Eng* 305:89–110
 101. Kochmann J, Brepols T, Wulfinghoff S, Svendsen B, Reese S (2018) On the computation of the exact overall consistent tangent moduli for non-linear finite strain homogenization problems using six finite perturbations. In: 6th European conference on computational mechanics (ECCM 6)
 102. Kochmann J, Ehle L, Wulfinghoff S, Mayer J, Svendsen B, Reese S (2018) Efficient multiscale FE-FFT-based modeling and simulation of macroscopic deformation processes with non-linear heterogeneous microstructures. In: *Multiscale modeling of heterogeneous structures*. Springer, Cham, pp. 129–146
 103. Kochmann J, Wulfinghoff S, Ehle L, Mayer J, Svendsen B, Reese S (2018) Efficient and accurate two-scale FE-FFT-based prediction of the effective material behavior of elasto-viscoplastic polycrystals. *Comput Mech* 61:751–764
 104. Kochmann J, Manjunatha K, Gierden C, Wulfinghoff S, Svendsen B, Reese S (2019) A simple and flexible model order reduction method for FFT-based homogenization problems using a sparse sampling technique. *Comput Methods Appl Mech Eng* 347:622–638
 105. Kouznetsova V, Brekelmans WAM, Baaijens FT (2001) An approach to micro-macro modeling of heterogeneous materials. *Comput Mech* 27:37–48
 106. Kröner E (1958) Berechnung der elastischen Konstanten des Vielkristalls aus den Konstanten des Einkristalls. *Z Phys* 151:504–518
 107. Kröner E (1972) *Statistical continuum mechanics*, vol 92. Springer, Vienna
 108. Kumar MA, Kanjarla AK, Niezgoda SR, Lebensohn RA, Tomé CN (2015) Numerical study of the stress state of a deformation twin in magnesium. *Acta Mater* 84:349–358
 109. Kumar MA, Beyerlein IJ, Tomé CN (2016) Effect of local stress fields on twin characteristics in HCP metals. *Acta Mater* 116:143–154
 110. Lahellec N, Michel JC, Moulinec H, Suquet P (2003) Analysis of inhomogeneous materials at large strains using fast Fourier transforms. In: *IUTAM symposium on computational mechanics of solid materials at large strains, solid mechanics and its applications*, vol 108, pp 247–258
 111. Lavergne F, Sab K, Sanahuja J, Bornert M, Toulemonde C (2015) Investigation of the effect of aggregates' morphology on concrete creep properties by numerical simulations. *Cem Concr Res* 71:14–28
 112. Lebensohn RA (2001) N-site modeling of a 3D viscoplastic polycrystal using fast Fourier transform. *Acta Mater* 49:2723–2737
 113. Lebensohn RA, Needleman A (2016) Numerical implementation of non-local polycrystal plasticity using fast Fourier transforms. *J Mech Phys Solids* 97:333–351
 114. Lee SB, Lebensohn RA, Rollett AD (2011) Modeling the viscoplastic micromechanical response of two-phase materials using fast Fourier transforms. *Int J Plasticity* 27(5):707–727
 115. Lebensohn RA, Rollett AD (2020) Spectral methods for full-field micromechanical modelling of polycrystalline materials. *Comput Mater Sci* 173:109336
 116. Lebensohn RA, Tomé CN (1993) A self-consistent anisotropic approach for the simulation of plastic deformation and texture development of polycrystals: application to zirconium alloys. *Acta Metall Mater* 41(9):2611–2624

117. Lebensohn RA, Liu Y, Castañeda PP (2004) On the accuracy of the self-consistent approximation for polycrystals: comparison with full-field numerical simulations. *Acta Mater* 52(18):5347–5361
118. Lebensohn RA, Brenner R, Castelnau O, Rollett AD (2008) Orientation image-based micromechanical modelling of sub-grain texture evolution in polycrystalline copper. *Acta Mater* 56(15):3914–3926
119. Lebensohn RA, Montagnat M, Mansuy P, Duval P, Meysonnier J, Philip A (2009) Modeling viscoplastic behavior and heterogeneous intracrystalline deformation of columnar ice polycrystals. *Acta Mater* 57(5):1405–1415
120. Lebensohn RA, Castañeda PP, Brenner R, Castelnau O (2011) Full-field vs. homogenization methods to predict microstructure–property relations for polycrystalline materials. In: *Computational methods for microstructure–property relations*. Springer, Boston, pp 393–441
121. Lebensohn RA, Rollett AD, Suquet P (2011) Fast fourier transform-based modeling for the determination of micromechanical fields in polycrystals. *J Miner Met Mater Soc* 63(3):13–18
122. Lebensohn RA, Kanjarla AK, Eisenlohr P (2012) An elasto-viscoplastic formulation based on fast Fourier transforms for the prediction of micromechanical fields in polycrystalline materials. *Int J Plasticity* 32–33:59–69
123. Lebensohn RA, Escobedo JP, Cerreta EK, Dennis-Koller D, Bronkhorst CA, Bingert JF (2013) Modeling void growth in polycrystalline materials. *Acta Mater* 61(18):6918–6932
124. Leute RJ, Ladecký M, Falsafi A, Jödicke I, Pultarová I, Zeman J, Junge T, Pastewka L (2021) Elimination of ringing artifacts by finite-element projection in FFT-based homogenization. [arXiv:2105.03297](https://arxiv.org/abs/2105.03297)
125. Li S, Wang G (2008) *Introduction to Micromechanics and Nanomechanics*. World Scientific
126. Li MY, Cao YJ, Shen WQ, Shao JF (2017) A damage model of mechanical behavior of porous materials: application to sandstone. *Int J Damage Mech* 27(9):1325–1351
127. Lielens G, Pirotte P, Couniot A, Dupret F, Keunings R (1998) Prediction of thermo-mechanical properties for compression moulded composites. *Compos Res A Appl Sci Manuf* 29(1–2):63–70
128. Liu X, Shapiro V (2016) Homogenization of material properties in additively manufactured structures. *Comput Aid Des* 78:71–82
129. Liu B, Raabe D, Roters F, Eisenlohr P, Lebensohn RA (2010) Comparison of finite element and fast Fourier transform crystal plasticity solvers for texture prediction. *Model Simul Mater Sci Eng* 18(8):085005
130. Liu Z, Bessa MA, Liu WK (2016) Self-consistent clustering analysis: an efficient multi-scale scheme for inelastic heterogeneous materials. *Comput Methods Appl Mech Eng* 306:319–341
131. Liu Z, Fleming M, Liu WK (2018) Microstructural material database for self-consistent clustering analysis of elastoplastic strain softening materials. *Comput Methods Appl Mech Eng* 330:547–577
132. Liu PW, Wang Z, Xiao YH, Lebensohn RA, Liu YC, Horstemeyer MF, Cui XY, Chen L (2020) Integration of phase-field model and crystal plasticity for the prediction of process-structure-property relation of additively manufactured metallic materials. *Int J Plasticity* 128:102670
133. Lucarini S, Segurado J (2019) On the accuracy of spectral solvers for micromechanics based fatigue modeling. *Comput Mech* 63:365–382
134. Lucarini S, Upadhyay MV, Segurado J (2022) FFT based approaches in micromechanics: fundamentals, methods and applications. *Model Simul Mater Sci Eng* 30:023002
135. Ma R, Sun W (2020) FFT-based solver for higher-order and multi-phase-field fracture models applied to strongly anisotropic brittle materials. *Comput Methods Appl Mech Eng* 362:112781
136. Magri M, Lucarini S, Lemoine G, Adam L, Segurado J (2021) An FFT framework for simulating non-local ductile failure in heterogeneous materials. *Comput Methods Appl Mech Eng* 380:113759
137. Mandel J (1972) *Plasticité classique et viscoplasticité*. CISM lecture notes, vol 97. Springer, Berlin
138. Mareau C (2020) A non-local damage model for the fatigue behaviour of metallic polycrystals. *Philos Mag* 100(8):955–981
139. Marino M, Hudobivnik B, Wriggers P (2019) Computational homogenization of polycrystalline materials with the Virtual Element Method. *Comput Methods Appl Mech Eng* 355:349–372
140. Markovsky I (2012) *Low rank approximation*. Springer, London
141. Michel JC, Suquet P (2003) Nonuniform transformation field analysis. *Int J Solids Struct* 40(25):6937–6955
142. Michel JC, Suquet P (2004) Computational analysis of non-linear composite structures using the nonuniform transformation field analysis. *Comput Methods Appl Mech Eng* 193(48–51):5477–5502
143. Michel JC, Suquet P (2016) A model-reduction approach in micromechanics of materials preserving the variational structure of constitutive relations. *J Mech Phys Solids* 90:254–285
144. Michel JC, Moulinec H, Suquet P (1999) Effective properties of composite materials with periodic microstructure: a computational approach. *Comput Methods Appl Mech Eng* 172(1–4):109–143
145. Michel JC, Moulinec H, Suquet P (2000) A computational method based on augmented Lagrangians and fast Fourier transforms for composites with high contrast. *Comput Model Eng Sci* 1(2):79–88
146. Michel JC, Moulinec H, Suquet P (2001) A computational scheme for linear and non-linear composites with arbitrary phase contrast. *Int J Numer Methods Eng* 52(1–2):139–160
147. Miehe C (1996) Numerical computation of algorithmic (consistent) tangent moduli in large-strain computational inelasticity. *Comput Methods Appl Mech Eng* 134:223–240
148. Miehe C, Schröder J, Schotte J (1999) Computational homogenization analysis in finite plasticity simulation of texture development in polycrystalline materials. *Comput Methods Appl Mech Eng* 171(3–4):387–418
149. Miehe C, Schröder J, Schotte J (1999) Computational micro-macro transitions and overall moduli in the analysis of polycrystals at large strains. *Comput Mater Sci* 16:372–382
150. Miehe C, Schotte J, Lambrecht M (2002) Homogenization of inelastic solid materials at finite strains based on incremental minimization principles. Application to the texture analysis of polycrystals. *J Mech Phys Solids* 50(10):2123–2167
151. Molinari A, Canova GR, Ahzi S (1987) A self consistent approach of the large deformation polycrystal viscoplasticity. *Acta Metall* 35:2983–2994
152. Monchiet V, Bonnet G (2012) A polarization-based FFT iterative scheme for computing the effective properties of elastic composites with arbitrary contrast. *Int J Numer Methods Eng* 89(11):1419–1436
153. Mori T, Tanaka K (1973) Average stress in matrix and average elastic energy of materials with misfitting inclusions. *Acta Metall* 21(5):571–574
154. Moulinec H, Silva F (2014) Comparison of three accelerated FFT-based schemes for computing the mechanical response of composite materials. *Int J Numer Methods Eng* 97:960–985
155. Moulinec H, Suquet P (1994) A fast numerical method for computing the linear and nonlinear mechanical properties of composites. *Compt Rend Acad Sci Sér II Méc Phys Chim Astron* 318(11):1417–1423

156. Moulinec H, Suquet P (1998) A numerical method for computing the overall response of nonlinear composites with complex microstructure. *Comput Methods Appl Mech Eng* 157(1–2):69–94
157. Moulinec H, Suquet P (2003) Comparison of FFT-based methods for computing the response of composites with highly contrasted mechanical properties. *Physica B Condens Matter* 338(1–4):58–60
158. Mura T (1987) Micromechanics of defects in solids. In: *Mechanics of elastic and inelastic solids*, vol 3. Springer, Dordrecht
159. Nemat-Nasser S, Hori M (1998) *Micromechanics: overall properties of heterogeneous materials*. North Holland, Amsterdam
160. Niezgodá SR, Kanjarla AK, Beyerlein IJ, Tomé CN (2014) Stochastic modeling of twin nucleation in polycrystals: an application in hexagonal close-packed metals. *Int J Plasticity* 56:119–138
161. Ostoja-Starzewski M (2002) Towards stochastic continuum thermodynamics. *J Non-Equilib Thermodyn* 27:335–348
162. Ostrowski K, Stefaniuk D, Sadowski L, Krzywiński K, Gicala M, Rózańska M (2020) Potential use of granite waste sourced from rock processing for the application as coarse aggregate in high-performance self-compacting concrete. *Constr Build Mater* 238:117794
163. Ozturk T, Rollett AD (2018) Effect of microstructure on the elasto-viscoplastic deformation of dual phase titanium structures. *Comput Mech* 61:55–70
164. Petch NJ (1953) The cleavage strength of polycrystals. *J Iron Steel Inst* 174:25–28
165. Pinnau R (2008) *Model reduction via proper orthogonal decomposition*, vol 13. Springer, Cham
166. Pokharel R, Lind J, Kanjarla AK, Lebensohn RA, Li SF, Kenesei P, Suter RM, Rollett AD (2014) Polycrystal plasticity: comparison between grain-scale observations of deformation and simulations. *Annu Rev Condens Matter Phys* 5:317–346
167. Prakash A, Lebensohn RA (2009) Simulations of micromechanical behavior of polycrystals: finite elements versus fast Fourier transforms. *Model Simul Mater Sci Eng* 17(6):064010
168. Rambašek M, Göküzüm FS, Nguyen LTK, Keip MA (2019) A two-scale FE-FFT approach to nonlinear magneto-elasticity. *Int J Numer Methods Eng* 117(11):1117–1142
169. Reuss A (1929) Berechnung der Fließgrenze von Mischkristallen auf Grund der Plastizitätsbedingung für Einkristalle. *ZAMM J Appl Math Mech* 9(1):49–58
170. Rezaei S, Jaworek D, Mianroodi JR, Wulfinghoff S, Reese S (2019) Atomistically motivated interface model to account for coupled plasticity and damage at grain boundaries. *J Mech Phys Solids* 124:325–349
171. Rollett AD, Lebensohn RA, Groeber M, Choi Y, Li J, Rohrer GS (2010) Stress hot spots in viscoplastic deformation of polycrystals. *Model Simul Mater Sci Eng* 18(7):074005
172. Roters F, Diehl M, Shanthraj P, Eisenlohr P, Reuber C, Wong SL, Maiti T, Ebrahimi A, Hochrainer T, Fabritius HO, Nikolov S, Friák M, Fujita N, Grilli N, Janssens KGF, Jia N, Kok PJJ, Ma D, Meier F, Werner E, Stricker M, Weygand D, Raabe D (2019) DAMASK - The Düsseldorf Advanced Material Simulation Kit for modeling multi-physics crystal plasticity, thermal, and damage phenomena from the single crystal up to the component scale. *Comput Mater Sci* 158:420–478
173. Roters F, Eisenlohr P, Hantcherli L, Tjahjanto DD, Bieler TR, Raabe D (2010) Overview of constitutive laws, kinematics, homogenization and multiscale methods in crystal plasticity finite-element modeling: theory, experiments, applications. *Acta Mater* 58(4):1152–1211
174. Roters F, Eisenlohr P, Kords C, Tjahjanto DD, Diehl M, Raabe D (2012) DAMASK: the Düsseldorf Advanced Material Simulation Kit for studying crystal plasticity using an FE based or a spectral numerical solver. *Procedia IUTAM* 3:3–10
175. Rovinelli A, Guilhem Y, Proudhon H, Lebensohn RA (2017) Assessing reliability of fatigue indicator parameters for small crack growth via a probabilistic framework. *Model Simul Mater Sci Eng* 25:045010
176. Rovinelli A, Sangid MD, Proudhon H, Guilhem Y, Lebensohn RA, Ludwig W (2018) Predicting the 3D fatigue crack growth rate of small cracks using multimodal data via Bayesian networks: In-situ experiments and crystal plasticity simulations. *J Mech Phys Solids* 115:208–229
177. Sachs G (1929) Zur Ableitung einer Fließbedingung. *Mitteilungen der deutschen Materialprüfungsanstalten* 72:94–97
178. Santos-Güemes R, Esteban-Manzanares G, Papadimitriou I, Segurado J, Capolungo L, LLorca J (2018) Discrete dislocation dynamics simulations of dislocation- θ' precipitate interaction in Al-Cu alloys. *J Mech Phys Solids* 118:228–244
179. Schneider M (2017) An FFT-based fast gradient method for elastic and inelastic unit cell homogenization problems. *Comput Methods Appl Mech Eng* 315:846–866
180. Schneider M (2019) On the Barzilai-Borwein basic scheme in FFT-based computational homogenization. *Int J Numer Methods Eng* 118(8):482–494
181. Schneider M (2021) A review of nonlinear FFT-based computational homogenization methods. *Acta Mech* 232:2051–2100
182. Schneider M, Ospald F, Kabel M (2016) Computational homogenization of elasticity on a staggered grid. *Int J Numer Methods Eng* 105(9):693–720
183. Schneider M, Merkert D, Kabel M (2017) FFT-based homogenization for microstructures discretized by linear hexahedral elements. *Int J Numer Methods Eng* 109(10):1461–1489
184. Schneider M, Wicht D, Böhlke T (2019) On polarization-based schemes for the FFT-based computational homogenization of inelastic materials. *Comput Mech* 64:1073–1095
185. Schröder J (2000) *Homogenisierungsmethoden der nichtlinearen Kontinuumsmechanik unter Beachtung von Instabilitäten*. Universität Stuttgart, Institut für Mechanik (Bauwesen), Habilitation
186. Schröder J, Hackl K (2014) Plasticity and beyond—microstructures, crystal plasticity and phase transitions. In: *CISM international centre for mechanical sciences*, vol 550. Springer, Vienna
187. Segurado J, Lebensohn RA, LLorca J, Tomé CN (2012) Multi-scale modeling of plasticity based on embedding the viscoplastic self-consistent formulation in implicit finite elements. *Int J Plasticity* 28(1):124–140
188. Segurado J, Lebensohn RA, LLorca J (2018) Computational homogenization of polycrystals. *Adv Appl Mech* 51:1–114
189. Shanthraj P, Eisenlohr P, Diehl M, Roters F (2015) Numerically robust spectral methods for crystal plasticity simulations of heterogeneous materials. *Int J Plasticity* 66:31–45
190. Sharma L, Peerlings RHJ, Shanthraj P, Roters F, Geers MGD (2018) FFT-based interface decohesion modelling by a nonlocal interphase. *Adv Model Simul Eng Sci* 5(1):1–17
191. Sharma L, Peerlings RHJ, Shanthraj P, Roters F, Geers MGD (2020) An FFT-based spectral solver for interface decohesion modelling using a gradient damage approach. *Comput Mech* 65:925–939
192. Sliseris J, Andrä H, Kabel M, Bix B, Plinke B, Wirjadi O, Frolovs G (2014) Numerical prediction of the stiffness and strength of medium density fiberboards. *Mech Mater* 79:73–84
193. Šmilauer V, Bažant ZP (2010) Identification of viscoelastic C–S–H behavior in mature cement paste by FFT-based homogenization method. *Cem Concr Res* 40(2):197–207
194. Smit RJM, Brekelmans WAM, Meijer HEH (1998) Prediction of the mechanical behavior of nonlinear heterogeneous systems

- by multi-level finite element modeling. *Comput Methods Appl Mech Eng* 155(1–2):181–192
195. Song D, Castañeda PP (2018) Fully optimized second-order homogenization estimates for the macroscopic response and texture evolution of low-symmetry viscoplastic polycrystals. *Int J Plasticity* 110:272–293
 196. Spahn J, Andrä H, Kabel M, Müller R (2014) A multiscale approach for modeling progressive damage of composite materials using fast Fourier transforms. *Comput Methods Appl Mech Eng* 268:871–883
 197. Suquet P (1997) Continuum micromechanics. In: CISM international center for mechanical sciences, vol 377. Springer, Vienna
 198. Suquet P, Moulinec H, Castelnau O, Montagnat M, Lahellec N, Grennerat F, Duval P, Brenner R (2012) Multi-scale modeling of the mechanical behavior of polycrystalline ice under transient creep. *Procedia IUTAM* 3:76–90
 199. Talbot DRS, Willis JR (1985) Variational principles for inhomogeneous non-linear media. *IMA J Appl Math* 35(1):39–54
 200. Talbot DRS, Willis JR (1987) Bounds and self-consistent estimates for the overall properties of nonlinear composites. *IMA J Appl Math* 39(3):215–240
 201. Tari V, Lebensohn RA, Pokharel R, Turner TJ, Shade PA, Bernier JV, Rollett AD (2018) Validation of micro-mechanical FFT-based simulations using High Energy Diffraction Microscopy on Ti–7Al. *Acta Mater* 154:273–283
 202. Tasan CC, Diehl M, Yan D, Zambaldi C, Shanthraj P, Roters F, Raabe D (2014) Integrated experimental-simulation analysis of stress and strain partitioning in multiphase alloys. *Acta Mater* 81:386–400
 203. Taylor GI (1938) Plastic strain in metals. *J Inst Met* 62:307–324
 204. Terada K, Kikuchi N (2001) A class of general algorithms for multi-scale analyses of heterogeneous media. *Comput Methods Appl Mech Eng* 190(40–41):5427–5464
 205. Torquato S (2002) Random heterogeneous materials: microstructure and macroscopic properties, Interdisciplinary applied mathematics, vol 16. Springer, New York
 206. Upadhyay MV, Petegem SV, Panzner T, Lebensohn RA, Swygenhoven HV (2016) Study of lattice strain evolution during biaxial deformation of stainless steel using a finite element and fast Fourier transform based multi-scale approach. *Acta Mater* 118:28–43
 207. Upadhyay MV, Capek J, Petegem SV, Lebensohn RA, Swygenhoven HV (2017) Intergranular strain evolution during biaxial loading: a multiscale FE-FFT approach. *J Miner Met Mater Soc* 69:839–847
 208. Upadhyay MV, Patra A, Wen W, Panzner T, Petegem SV, Tomé CN, Lebensohn RA, Swygenhoven HV (2018) Mechanical response of stainless steel subjected to biaxial load path changes: cruciform experiments and multi-scale modeling. *Int J Plasticity* 108:144–168
 209. Upadhyay MV, Capek J, Panzner T, Swygenhoven HV (2019) Microstructure evolution of stainless steel subjected to biaxial load path changes: in-situ neutron diffraction and multi-scale modeling. *Int J Plasticity* 122:49–72
 210. van der Sluis O, Schreurs PJG, Brekelmans WAM, Meijer HEH (2000) Overall behaviour of heterogeneous elastoviscoplastic materials: effect of microstructural modelling. *Mech Mater* 32(8):449–462
 211. Vidyasagar A, Tan WL, Kochmann DM (2017) Predicting the effective response of bulk polycrystalline ferroelectric ceramics via improved spectral phase field methods. *J Mech Phys Solids* 106:133–151
 212. Vidyasagar A, Tutcuoglu AD, Kochmann DM (2018) Deformation patterning in finite-strain crystal plasticity by spectral homogenization with application to magnesium. *Comput Methods Appl Mech Eng* 335:584–609
 213. Vinogradov V, Milton GW (2008) An accelerated FFT algorithm for thermoelastic and non-linear composites. *Int J Numer Methods Eng* 76(11):1678–1695
 214. Voigt W (1889) Annalen der Physik. Über die Beziehung zwischen den beiden Elastizitätskonstanten isotroper Körper. *Ann Phys* 38:573–587
 215. Volterra V (1907) Sur l'équilibre des corps élastiques multiplement connexes. *Ann Sci École Norm Sup* 24:401–517
 216. Vondřejc J (2016) Improved guaranteed computable bounds on homogenized properties of periodic media by the Fourier–Galerkin method with exact integration. *Int J Numer Methods Eng* 107(13):1106–1135
 217. Vondřejc J, Geus TWJ (2020) Energy-based comparison between the Fourier–Galerkin method and the finite element method. *J Comput Appl Math* 374:112585
 218. Vondřejc J, Zeman J, Marek I (2014) An FFT-based Galerkin method for homogenization of periodic media. *Comput Math Appl* 68(3):156–173
 219. Vondřejc J, Zeman J, Marek I (2015) Guaranteed upper-lower bounds on homogenized properties by FFT-based Galerkin method. *Comput Methods Appl Mech Eng* 297:258–291
 220. Vondřejc J, Liu D, Ladecký M, Matthies HG (2020) FFT-based homogenisation accelerated by low-rank tensor approximations. *Comput Methods Appl Mech Eng* 364:112890
 221. Waimann J, Gierden C, Schmidt A, Svendsen B, Reese S (2021) Microstructure simulation using self-consistent clustering analysis. *Proc Appl Math Mech* 20(1):e202000263
 222. Wang B, Fang G, Liu S, Fu M, Liang J (2018) Progressive damage analysis of 3D braided composites using FFT-based method. *Compos Struct* 192:255–263
 223. Wang B, Fang G, Liang J, Liu S, Meng S (2020) Efficient multiscale analysis method for the compressive progressive damage of 3D braided composites based on FFT. *Acta Mech* 231:5047–5061
 224. Welschinger F, Köbler J, Andrä H, Müller R, Schneider M, Staub S (2019) Efficient multiscale methods for viscoelasticity and fatigue of short fiber-reinforced polymers. *Key Eng Mater* 809:473–479
 225. Wicht D, Schneider M, Böhlke T (2020) An efficient solution scheme for small-strain crystal-elasto-viscoplasticity in a dual framework. *Comput Methods Appl Mech Eng* 358:112611
 226. Wicht D, Schneider M, Böhlke T (2020) On Quasi-Newton methods in fast Fourier transform-based micromechanics. *Int J Numer Methods Eng* 121(8):1665–1694
 227. Willis JR (1977) Bounds and self-consistent estimates for the overall properties of anisotropic composites. *J Mech Phys Solids* 25(3):185–202
 228. Willis JR (1981) Variational and related methods for the overall properties of composites. *Adv Appl Mech* 21:1–78
 229. Willot F (2015) Fourier-based schemes for computing the mechanical response of composites with accurate local fields. *Compt Rend Méc* 343(3):232–245
 230. Willot F, Abdallah B, Pellegrini YP (2014) Fourier-based schemes with modified Green operator for computing the electrical response of heterogeneous media with accurate local fields. *Int J Numer Methods Eng* 98(7):518–533
 231. Wulfinghoff S, Cavaliere F, Reese S (2018) Model order reduction of nonlinear homogenization problems using a Hashin–Shtrikman type finite element method. *Comput Methods Appl Mech Eng* 330:149–179
 232. Yu C, Kafka OL, Liu WK (2019) Self-consistent clustering analysis for multiscale modeling at finite strains. *Comput Methods Appl Mech Eng* 349:339–359
 233. Zeman J, Vondřejc J, Novák J, Marek I (2010) Accelerating a FFT-based solver for numerical homogenization of periodic media by conjugate gradients. *J Comput Phys* 229(21):8065–8071

234. Zeman J, de Geus TWJ, Vondřejc J, Peerlings RHJ, Geers MGD (2017) A finite element perspective on nonlinear FFT-based micromechanical simulations. *Int J Numer Methods Eng* 111(10):903–926
235. Zhang H, Diehl M, Roters F, Raabe D (2016) A virtual laboratory using high resolution crystal plasticity simulations to determine the initial yield surface for sheet metal forming operations. *Int J Plasticity* 80:111–138
236. Zhao P, Low TSE, Wang Y, Niezgoda SR (2016) An integrated full-field model of concurrent plastic deformation and microstructure evolution: application to 3D simulation of dynamic recrystallization in polycrystalline copper. *Int J Plasticity* 80:38–55
237. Zienkiewicz OC, Taylor RL (2000) *The finite element method, vol 2: solid mechanics*. McGraw-Hill, New York

Publisher's Note Springer Nature remains neutral with regard to jurisdictional claims in published maps and institutional affiliations.